J. Fluid Mech. (2001), *vol.* 427, *pp.* 359–388. Printed in the United Kingdom

Görtler vortices in compressible mixing layers

By J. M. SARKIES AND S. R. OTTO

School of Mathematics and Statistics, The University of Birmingham, Edgbaston, Birmingham, B15 2TT, UK

(Received 8 July 1998 and in revised form 13 July 2000)

In experiments, Plesniak, Mehta & Johnson (1994) have noted that curved two-stream mixing layers are susceptible to centrifugal instabilities under the condition that the slower of the streams curves towards the faster one; this condition is analogous to the concave curvature condition for the stability of the flow over a plate. The modes which arise manifest themselves as vortices aligned with the dominant flow direction. Previous numerical and analytical work has elucidated the structure of these vortices within incompressible mixing layers; Otto, Jackson & Hu (1996). In this paper we go on to investigate the rôles of compressibility and heating in determining the streamwise fate of Görtler vortices within these situations.

The development of the disturbances is monitored downstream and curves of neutral stability are plotted. The effect of changing the Mach number and free-stream temperatures is studied in detail. It is found that for certain parameter régimes modes can occur within convexly curved, or 'stable' mixing layers; these 'thermal modes' have no counterpart within incompressible mixing layers. By making use of a large Görtler number analysis we are able to verify our numerical results, and derive a very simple condition which yields information about the parameter ranges for which certain modes are likely to occur. As an aside this method can be used to show that no degree of wall cooling will allow sustained growth of Görtler vortices within boundary layers over convex plates.

1. Introduction

It has been seen in numerous studies that the rôle of compressibility is important in many flow situations; Gutmark, Schadow & Yu (1995) and Mack (1984). The flow in high-powered jet engines, involving the mixing of fuel and air, is one specific case. The inclusion of compressibility effects when studying these fluid flows naturally increases the complexity of the resulting systems. For certain parameter régimes formal asymptotic reductions can be used to generate relatively simple eigenvalue problems. However, there are certain situations where no suitable asymptotic framework can be determined, and in these problems recourse needs to be made to numerical methods.

Plesniak, Mehta & Johnson (1994, 1996) investigated curved two-stream mixing layers and they showed that the presence of centrifugal force promoted the evolution of streamwise vortices (the reader is referred to the other numerous experimental studies cited in these articles). Experiments were carried out with both initially untripped and tripped turbulent boundary layers. Only the untripped case exhibited sustained organized streamwise vorticity. The higher growth rate of the mixing layer seen in this case is attributed to the presence of spatially stationary streamwise vortices, which

are seen to provide extra entrainment, as Bell & Mehta (1990) showed for a plane mixing layer.

Due to the natural shape of their velocity profiles, mixing layers can sustain inviscid travelling-wave instabilities. It is known that these inflectionally driven modes occur almost instantaneously downstream of a splitter plate and will cause the two streams to start mixing, Karasso & Mungal (1997). One interesting question is whether centrifugal effects can promote mixing, either directly or via the modification of the inherent inviscid modes, Otto (1995).

The occurrence of streamwise vortices within boundary layers on concave plates was initially predicted by Görtler (1940). The modes take the form of pairs of streamwise-orientated counter-rotating vortices which are self-evidently periodic in the spanwise direction. Görtler and many other subsequent authors fallaciously considered the underlying flow to be independent of the downstream coordinate. The full inclusion of non-parallel flow effects was first presented by Hall (1982), where a formal asymptotic framework was laid down. Therein the normal and spanwise coordinates were rescaled on the thickness of the boundary layer in order to capture the vortex mechanism. The Görtler number, a parameter representing the level of centrifugal effects, is introduced and defined to be $G = 2\delta Re^{1/2}$, with δ a measure of curvature of the layer and Re the Reynolds number defined in the usual way (we take $Re \gg 1$). It is assumed that δ is sufficiently small so that as the Reynolds number increases, the Görtler number is fixed and of order one. Hall (1982) considered the large-G limit but with $G \ll Re$. As the modes evolve downstream they are known to maintain their spanwise wavelength, $(1/a)$, and hence it is pertinent to consider a high-wavenumber limit when normalizing with respect to the layer thickness.

In order to characterize the overall stability of a flow it is necessary to describe the shape of the neutral curve; this determines when a mode will be unstable. We can use an asymptotic analysis to determine the location of the right-hand branch of the neutral curve, which is a good gauge of the stability of a situation. The extent of the gap between the right- and left-hand branches of the neutral curve is equivalent to the coalescence or otherwise of the upper and lower branches of a Tollmien–Schlichting neutral curve for large Reynolds numbers. The fact that a flow is inviscidly unstable implies that the upper and lower branches are distinct which is congruous to the circulation condition derived herein. It is known that the right-hand branch of the neutral curve is characterized by $G \sim a^4$. An expansion for the Görtler number in terms of the wavenumber was found by Hall, and this was continued to the point at which non-parallel effects first appeared. The right-hand branch asymptote was compared to previous parallel-flow approximations and experimental findings; Hall (1982).

For the $O(1)$ scaled wavenumber problem (that is modes with wavelengths comparable with the boundary-layer thickness) with $G = O(1)$ also, there is no suitable reduction of the equations, which means that one is required to solve the full system of partial differential equations, as opposed to ordinary differential equations. For this régime, Hall (1983) numerically tracked the progress of the modes downstream within a Blasius boundary layer over a concave curved plate. If the curvature of the plate was convex it was found that the square of the circulation does not decrease anywhere as you move away from the plate (Rayleigh's circulation criterion) and thus there is no centrifugal instability. The effect of changing the initial form and location of the disturbance was investigated, and it was found that the structure far downstream remained unchanged. It was also seen that no unique neutral curve existed, which demonstrates the difficulty experienced in achieving repeatability in

experiments for Görtler vortices, Swearingen & Blackwelder (1987). The asymptotic results of Hall (1982) were plotted against the right-hand branch of the neutral curves, and good agreement was obtained. The corresponding compressible investigation was carried out by Wadey (1992), wherein the effect of wall cooling was investigated. It was seen that the right-hand branch of the neutral curve moved to the left as the wall was cooled; see Elliott & Bassom (2000) for a full account of the rôle of wall cooling in determining the structure of Görtler vortices. An increase in free-stream Mach number also moved the right-hand branch of the neutral curve to the left, thus diminishing the range over which modes are unstable.

The régime $G \gg 1$ and $a = O(1)$ was investigated by Denier, Hall & Seddougui (1991) for an incompressible boundary layer. It was found that inviscid Görtler vortices could be sustained within this flow situation. The corresponding compressible study was carried out by Dando & Seddougui (1991). Here it was found that different types of instability modes existed. There was a wall-layer mode, and for large Mach numbers a mode was shown to exist in a temperature adjustment layer. It has been seen in these compressible studies that an increase in the Mach number of the flow tended to lead to a more stable flow. This is a result that is in common with the majority of compressible flows which are susceptible to Tollmien–Schlichting instabilities, Mack (1984) (see however Sarkies & Otto (1999) for a counter-example).

The evolution of centrifugal instabilities within curved incompressible mixing layers has been studied theoretically and numerically in many papers. Hu, Otto & Jackson (1994) and Liou (1994) showed that curvature had little effect on the inflectional Rayleigh modes. However, the presence of curvature permits an unstable three-dimensional mode which will become the prominent mode as the scaled streamwise wavenumber decreases (this corresponds to reverting to the centrifugal case for which this wavenumber is effectively zero). Otto, Jackson & Hu (1996) presented both an analytical and numerical study. The existence of unstable modes was shown to be largely dependent on the slower stream curving into the faster one. Vortices akin to these modes have been studied within the atmosphere, Scorer & Wilson (1963) and Scorer (1997). These structures arise within curved flows occurring due to gravity, Otto, Stott & Denier (1999): they are thought to be a possible mechanism for generating 'clear-air turbulence' within the atmosphere. The analytical part of Otto *et al.* (1996) was concerned with inviscid and viscous right-hand branch modes in a high Taylor/Görtler number régime. It was also noted that the fastest growing mode found by Denier *et al.* (1991) in the incompressible boundary-layer problem was not present in the curved mixing layer. In the numerical part of Otto *et al.* (1996) the parabolic vortex equations were integrated and marched in the downstream direction. The wavenumber was taken to have an $O(1)$ value, as was the Görtler number. It was found that as the difference between the free-stream speeds increased the layer became more susceptible to centrifugal instabilities. Growth of the modes was also observed when the mixing layer curves towards the slower stream, although the growth rate was positive for very short streamwise distances: this transient growth is commented upon in Plesniak *et al.* (1994). It was also seen that a change in the initial perturbation only served to alter the base of the neutral curves and not the ultimate downstream behaviour.

Owen, Seddougui & Otto (1997) completed a similar study to Hall (1982) (and also to the analytical part of Otto *et al.* 1996) for a compressible mixing layer. As well as finding modes that have counterparts in the incompressible problem herein referred to as 'conventional modes', Owen *et al.* (1997) found a new class of modes which do not exist in the incompressible problem; these 'thermal modes' arise when

a significantly cooler and slower stream curves away from a faster stream (which is analogous to convex curvature). It is worth noting that both of these classes of modes owe their existence to the presence of centrifugal force, the main difference being that the 'conventional modes' are driven by velocity shear, whereas the 'thermal modes' are sustained by thermal gradients. Plots showing the asymptotic location of the right-hand branch for changes in the Mach number and free-stream temperature ratio were given. These results are reproduced and extended in this paper to show agreement with numerical calculations. Similar modes have been shown to occur within shear layers with a deficit in velocity due to a wake component, Zhuang (1999), and in boundary and mixing layers where a degree of buoyancy is allowed, Stott & Denier (1998) and Otto *et al.* (1999).

We exploit the high-wavenumber limit of the inviscid problem to gain some very useful information pertaining to the ranges of free-stream temperature and velocity ratios for which these modes persist. It happens that the ratio of stream speeds used in most of Owen *et al.* (1997) was fortuitous. Far downstream, the modes become localized within a certain region, and Owen *et al.* (1997) determined where within the mixing layer this was located. This knowledge can be used to glean whether centrifugal instabilities could enhance or inhibit mixing. It was anticipated that if the mode resided around the centreline, then mixing would be enhanced.

In Owen, Seddougui & Otto (1998), which follows the incompressible study of Seddougui & Otto (1995), the nonlinear structure of the centrifugal instabilities was investigated. The calculation was affected in the parameter régime corresponding to the neighbourhood of the right-hand branch of the neutral curve. The nonlinear structure of the 'thermal modes' was given along with a consideration of the effect of the nonlinear modes on the inherent inviscid modes, Michalke (1964). It was found in both papers that the predominantly velocity-driven mode had the effect of reducing the temporal growth rates of the inviscid Rayleigh modes. However, Owen *et al.* (1998) found that the presence of the thermal modes produced a destabilization of the inviscid modes, see Otto, Sarkies & Denier (2000).

The focus of this paper is to investigate the effect of compressibility on centrifugal instabilities which are known to reside in curved compressible mixing layers. (Some preliminary work has been reported on in Sarkies & Otto 1998.) In § 2 the basic flow and the linear stability equations are formulated. In § 3 a summary of the asymptotic structures of the inviscid and the viscous right-hand branch modes is discussed. We include the derivation of a condition which can be used to predict when a situation will be prone to certain modes. Comparisons are made between the full numerical solutions and the asymptotic predictions in § 4. Finally, in § 5 we present our conclusions, and mention the work that has been undertaken as a natural extension of this study. Suggestions for other areas of future exploration are also discussed.

2. Formulation

2.1. *Basic flow*

The flow profile with which we are concerned occurs within a compressible mixing layer. This flow comprises two streams of different properties, meeting at the end of a splitter plate. It should be noted that not only may the two streams have differing velocities, but also different temperatures. We denote the velocity and temperature of the lower stream by $U_{-\infty}$ and $T_{-\infty}$ respectively, and those of the upper stream by

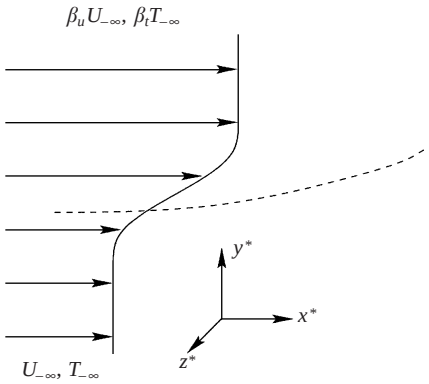

FIGURE 1. Schematic of the flow situation. In this article we shall consider $\beta_u > 1$ so that the upper stream is always the faster.

$\beta_u U_{-\infty}$ and $\beta_t T_{-\infty}$, figure 1. Our attention is restricted to $\beta_u > 1$ so that the upper stream is always faster; there is a simple correspondence with the results for $\beta_u < 1$.

The entire configuration is bounded above and below, with the width of the containing channel taken to be L. The Reynolds number is defined as $Re = U_{-\infty}L/\nu_{-\infty}$, where $\nu_{-\infty}$ is the kinematic viscosity of the lower stream. We exploit the dimensional coordinate system (x^*, y^*, z^*), where x^* is the distance along the centreline of the layer, y^* is normal to the centreline and z^* completes the orthogonal triad, see figure 1. The centreline of the mixing layer has curvature $(1/R)\chi(x^*/L)$, with R the radius of curvature. We use the convention that positive χ denotes a concave curvature (curving upwards), whereas negative χ implies a convex curvature (this being fixed by the geometry of the problem). The result of transforming into this coordinate system is the occurrence of extra terms in the normal-momentum equation. We define the Görtler number as in the introduction, with $\delta = L/R$. The assumption that $\delta \ll 1$ implies that the width of the containing channel is narrow compared to the radius of curvature.

To obtain the basic flow it is necessary to solve the energy, state, conservation of mass and compressible Navier–Stokes equations. The equation of state is taken to be that for an ideal gas. The thickness of the mixing layer, which is known to increase downstream, is $O(Re^{-1/2})$ and we rescale the normal velocity and lengthscale accordingly. The spanwise coordinate will also be rescaled as the Görtler vortex mechanism operates on a scale of $O(Re^{-1/2})$ in this direction.

The basic flow in a two-dimensional mixing layer takes the form

$$\boldsymbol{u} = U_{-\infty}[\bar{u}(x, y),\ Re^{-1/2}\bar{v}(x, y),\ 0][1 + O(Re^{-1/2})].$$

The bar denotes a basic-flow quantity and the rescaled coordinates are

$$x = x^*/L, \quad y = y^* Re^{1/2}/L, \quad z = z^* Re^{1/2}/L,$$

which are now in non-dimensional form. We also non-dimensionalize the density, viscosities, pressure and temperature with respect to their values in the lower stream, so that

$$\rho^* = \rho_{-\infty}\rho, \quad \mu^* = \mu_{-\infty}\mu, \quad \lambda^* = \lambda_{-\infty}\lambda,$$
$$p^* = \rho_{-\infty}U_{-\infty}^2 p, \quad T^* = T_{-\infty}T,$$

where an asterisk represents a dimensional quantity and λ is the second coefficient

of viscosity. This expresses to what extent the density changes with pressure, and is obtained from Stokes' relation, which in non-dimensional form is $\lambda + \frac{2}{3}\mu = 0$. We take $\bar{p} = 1/(\gamma M_{-\infty}^2)$ (with $M_{-\infty} = U_{-\infty}/a_{-\infty}$ the Mach number of the lower stream, where $a_{-\infty}$ is the speed of sound in the lower stream) so that $\bar{\rho}\,\bar{T} = 1$, from the equation of state. We also assume that the fluid obeys Chapman's linear viscosity law which relates temperature to viscosity ($\mu = c_H T$ in non-dimensional form). For this study Chapman's law was seen to be an adequate model for the temperature dependence of viscosity. However, for flows which are supersonic or hypersonic in nature, Sutherland's law may be more applicable. For a detailed discussion on the choice of viscosity model, the reader is referred to Blackaby (1991). Later in the study we take c_H to be unity for simplicity. This may have rendered the viscosity law slightly inaccurate in the cases where there are large temperature differences, see Rasmussen (1994). In these cases, it can be seen that in the relevant temperature range, the value of c_H can be chosen to match closely with Sutherland's law. This being the case, we do not see the use of Chapman's law as overly restrictive. We take the Prandtl number to be 0.72, which corresponds to air, although some use of a Prandtl number of unity is made in order to make analytical progress. (Numerical solutions are given for both values.)

To aid analysis we employ the Howarth–Dorodnitsyn transformation,

$$Y = \int_0^y \bar{\rho}(x, y)\,\mathrm{d}y,$$

which leads to equations that are in a similar form to those for an incompressible flow. Now, if we let $X = x$ we find that

$$\frac{\partial}{\partial x} \to \frac{\partial}{\partial X} + \frac{\partial Y}{\partial x}\frac{\partial}{\partial Y} \quad \text{and} \quad \frac{\partial}{\partial y} \to \bar{\rho}\frac{\partial}{\partial Y}.$$

We introduce the stream function $\psi(X, Y)$ such that

$$\bar{u} = \frac{\partial \psi}{\partial Y} \quad \text{and} \quad \bar{v} = -\frac{1}{\rho}\left(\frac{\partial \psi}{\partial X} + \frac{\partial Y}{\partial x}\bar{u}\right),$$

which implies that the conservation of mass equation is automatically satisfied. We look for self-similar solutions and accordingly define the similarity variable $\eta = Y/\sqrt{X}$, so that the spreading of the mixing layer is accounted for. The stream function is taken to be $\psi(X, \eta) = \sqrt{X}\,f(\eta)$. We note that

$$\frac{\partial Y}{\partial x} = \frac{1}{2\sqrt{X}\,\bar{T}}\int_0^\eta \tilde{\eta}\frac{\partial \bar{T}}{\partial \tilde{\eta}}\,\mathrm{d}\tilde{\eta},$$

as given in Stewartson (1964). The velocity components are now of the form

$$\bar{u} = \frac{\partial f}{\partial \eta} \quad \text{and} \quad \bar{v} = \frac{1}{2\sqrt{X}}\left\{\bar{T}\left(\eta\frac{\partial f}{\partial \eta} - f\right) - \frac{\partial f}{\partial \eta}\int_0^\eta \tilde{\eta}\frac{\partial \bar{T}}{\partial \tilde{\eta}}\,\mathrm{d}\tilde{\eta}\right\},$$

where f satisfies the Blasius equation

$$\frac{\partial^3 f}{\partial \eta^3} + \tfrac{1}{2} f\frac{\partial^2 f}{\partial \eta^2} = 0. \tag{1}$$

The above equation is solved in the region $(-\infty, \infty)$ and requires three boundary

conditions. Two of these arise from prescribing the streamwise velocities at $\pm\infty$:

$$\frac{\partial f}{\partial \eta}(\infty) = \beta_u \quad \text{and} \quad \frac{\partial f}{\partial \eta}(-\infty) = 1.$$

For the third boundary condition, Lock (1951) proposed that the normal velocity at the centreline should be zero, giving $f(0) = 0$ and Ting (1959) derived a set of boundary conditions by matching pressure terms to higher order across the mixing layer. In dimensional form, the condition mainly used here is given by

$$\frac{\bar{\rho}(\infty)\bar{u}(\infty)\bar{v}(\infty)}{\sqrt{1-M_\infty^2}} + \frac{\bar{\rho}(-\infty)\bar{u}(-\infty)\bar{v}(-\infty)}{\sqrt{1-M_{-\infty}^2}} = 0,$$

where $M_\infty = \beta_u M_{-\infty}/\sqrt{\beta_t}$ (this is the condition given in Ting (1959) applicable to the case of the combination of two subsonic streams). It was noted by Klemp & Acrivos (1972) that the analysis of Ting does not hold for a subsonic/subsonic mixing layer where the streams are semi-infinite in extent. In such a case the location of the dividing streamline is indeterminate. However, if the streams are bounded, the pressure across the mixing layer will not balance identically and a similar analysis to that presented by Ting (1959) will hold. Comments are given in Owen *et al.* (1997) on the effect of considering a Lock rather than a Ting boundary condition: the mode locations are found to be slightly shifted, but the growth rates remain largely unchanged.†

The temperature is found by integrating the energy equation and for arbitrary Prandtl number, σ, it is given by

$$\bar{T} = 1 + \mathscr{B}\int_{-\infty}^{\eta}\left(\frac{\partial^2 f}{\partial \eta^2}(\eta_1)\right)^{\sigma} \mathrm{d}\eta_1 - M_{-\infty}^2(\gamma-1)\sigma\int_{-\infty}^{\eta}\left(\frac{\partial^2 f}{\partial \eta^2}(\eta_1)\right)^{\sigma}\int_{-\infty}^{\eta_1}\left(\frac{\partial^2 f}{\partial \eta^2}(\eta_2)\right)^{2-\sigma}\mathrm{d}\eta_2\,\mathrm{d}\eta_1,$$

Stewartson (1964). It is noted that if the Prandtl number $\sigma = 1$, then the temperature can be found by considering the total enthalpy. Note also that for $\sigma > 2$ the above formula needs to be rewritten, effectively changing the order of integration in the final term. The constant $\mathscr{B}$ is obtained after applying the first of the two boundary conditions,

$$\bar{T}(\infty) = \beta_t, \qquad \bar{T}(-\infty) = 1,$$

and is found to be

$$\mathscr{B} = \left\{\beta_t - 1 + M_{-\infty}^2(\gamma-1)\sigma\int_{-\infty}^{\infty}\left(\frac{\partial^2 f}{\partial \eta^2}(\eta_1)\right)^{\sigma}\int_{-\infty}^{\eta_1}\left(\frac{\partial^2 f}{\partial \eta^2}(\eta_2)\right)^{2-\sigma}\mathrm{d}\eta_2\,\mathrm{d}\eta_1\right\}\Bigg/ \int_{-\infty}^{\infty}\left(\frac{\partial^2 f}{\partial \eta^2}(\eta_1)\right)^{\sigma}\mathrm{d}\eta_1.$$

The second boundary condition is satisfied by virtue of the choice of the lower limits of the integrals. We now proceed to introduce perturbations into the flow.

† It is worth noting at this point that many papers concerning mixing layers exploit the so-called 'hyperbolic tangent profile', for which

$$\bar{u} = \frac{\beta_u + 1}{2} + \frac{\beta_u - 1}{2}\tanh\eta,$$

and the temperature can be found in terms of the enthalpy.

2.2. *Disturbance equations*

The basic state is perturbed in such a way that we can investigate the susceptibility to centrifugal instabilities of curved compressible mixing layers. It is noted that the normal and spanwise coordinates are scaled on the mixing-layer thickness; the velocity components in these directions are also scaled. These rescalings result in terms representing the downstream evolution of the mixing layer being present at leading order in the equations. There is no reason to neglect these in favour of a parallel-flow approach, and thus a normal-mode investigation, such as that given in Floryan & Saric (1979) for incompressible flow over a concave plate, is not viable. It is noted from Plesniak *et al.* (1994) that the instabilities have a vortex structure and so the total flow, $\boldsymbol{u}_T$, is expressed in the form

$$\boldsymbol{u}_T = \boldsymbol{u} + \Delta[\tilde{u}(x,y), Re^{-1/2}\,\tilde{v}(x,y),\ Re^{-1/2}\,\tilde{w}(x,y)]\mathrm{e}^{\mathrm{i}az},$$

where Δ is a vanishingly small parameter, so that the resulting analysis is linear. The other flow quantities are perturbed in a similar manner so that

$$[p, T, \rho, \mu] = [\bar{p}, \bar{T}, \bar{\rho}, \bar{\mu}] + \Delta[Re^{-1}\tilde{p}(x,y),\ \tilde{T}(x,y),\ \tilde{\rho}(x,y),\ \tilde{\mu}(x,y)]\mathrm{e}^{\mathrm{i}az}.$$

Substituting these perturbations into the equations of motion and linearizing we arrive at the following disturbance equations:
conservation of mass

$$\frac{\partial}{\partial x}\left(\frac{\tilde{u}}{\bar{T}}\right) + \frac{\partial}{\partial y}\left(\frac{\tilde{v}}{\bar{T}}\right) + \frac{\mathrm{i}a}{\bar{T}}\tilde{w} - \frac{\partial}{\partial x}\left(\frac{\bar{u}\tilde{T}}{\bar{T}^2}\right) - \frac{\partial}{\partial y}\left(\frac{\bar{v}\tilde{T}}{\bar{T}^2}\right) = 0, \tag{2a}$$

streamwise momentum

$$\mathscr{L}_{1,1}(\tilde{u}) = \frac{\tilde{u}}{\bar{T}}\frac{\partial \bar{u}}{\partial x} + \frac{\tilde{v}}{\bar{T}}\frac{\partial \bar{u}}{\partial y} - \frac{\tilde{T}}{\bar{T}^2}\left(\bar{u}\frac{\partial \bar{u}}{\partial x} + \bar{v}\frac{\partial \bar{u}}{\partial y}\right) - \frac{\partial}{\partial y}\left(\tilde{T}\frac{\partial \bar{u}}{\partial y}\right), \tag{2b}$$

normal momentum

$$\begin{aligned}\mathscr{L}_{4/3,1}(\tilde{v}) = {} & \frac{\tilde{u}}{\bar{T}}\frac{\partial \bar{v}}{\partial x} + \frac{\tilde{v}}{\bar{T}}\frac{\partial \bar{v}}{\partial y} + \frac{\chi}{\bar{T}}G\bar{u}\tilde{u} - \frac{\tilde{T}}{\bar{T}^2}\left(\bar{u}\frac{\partial \bar{v}}{\partial x} + \bar{v}\frac{\partial \bar{v}}{\partial y} + \frac{\chi}{2}G\bar{u}^2\right) + \frac{\partial \tilde{p}}{\partial y} - \frac{\partial}{\partial x}\left(\bar{T}\frac{\partial \tilde{u}}{\partial y}\right) \\ & - \frac{\partial}{\partial x}\left(\tilde{T}\frac{\partial \bar{u}}{\partial y}\right) + \frac{\partial}{\partial y}\left(\frac{2}{3}\bar{T}\frac{\partial \tilde{u}}{\partial x} + \frac{2}{3}\bar{T}\mathrm{i}a\tilde{w}\right) + \frac{\partial}{\partial y}\left(\frac{2}{3}\tilde{T}\frac{\partial \bar{u}}{\partial x} - \frac{4}{3}\tilde{T}\frac{\partial \bar{v}}{\partial y}\right) - \mathrm{i}a\bar{T}\frac{\partial \tilde{w}}{\partial y},\end{aligned} \tag{2c}$$

spanwise momentum

$$\mathscr{L}_{1,4/3}(\tilde{w}) = \mathrm{i}a\tilde{p} - \frac{\partial}{\partial x}(\bar{T}\mathrm{i}a\tilde{u}) - \frac{\partial}{\partial y}(\bar{T}\mathrm{i}a\tilde{v}) + \frac{2}{3}\mathrm{i}a\bar{T}\left(\frac{\partial \tilde{u}}{\partial x} + \frac{\partial \tilde{v}}{\partial y}\right) + \frac{2}{3}\mathrm{i}a\tilde{T}\left(\frac{\partial \bar{u}}{\partial x} + \frac{\partial \bar{v}}{\partial y}\right), \tag{2d}$$

and energy

$$\begin{aligned}\mathscr{L}_{1/\sigma,1/\sigma}(\tilde{T}) = {} & \frac{\tilde{u}}{\bar{T}}\frac{\partial \bar{T}}{\partial x} + \frac{\tilde{v}}{\bar{T}}\frac{\partial \bar{T}}{\partial y} - \frac{\bar{u}\tilde{T}}{\bar{T}^2}\frac{\partial \bar{T}}{\partial x} - \frac{\bar{v}\tilde{T}}{\bar{T}^2}\frac{\partial \bar{T}}{\partial y} - \frac{1}{\sigma}\frac{\partial}{\partial y}\left(\tilde{T}\frac{\partial \bar{T}}{\partial y}\right) \\ & - M_{-\infty}^2(\gamma - 1)\left[\tilde{T}\left(\frac{\partial \bar{u}}{\partial y}\right)^2 + 2\bar{T}\frac{\partial \bar{u}}{\partial y}\frac{\partial \tilde{u}}{\partial y}\right],\end{aligned} \tag{2e}$$

where we have defined the operator

$$\mathscr{L}_{\alpha,\beta}(\phi) = \alpha\frac{\partial}{\partial y}\left(\bar{T}\frac{\partial\phi}{\partial y}\right) - \beta a^2\bar{T}\phi - \frac{\bar{u}}{\bar{T}}\frac{\partial\phi}{\partial x} - \frac{\bar{v}}{\bar{T}}\frac{\partial\phi}{\partial y}.$$

We have taken the Chapman constant, c_H, to be unity (as mentioned earlier, it may be pertinent in cases where large temperature gradients occur to choose a different value of c_H). The appropriate boundary conditions are

$$\tilde{u}, \tilde{v}, \frac{\partial\tilde{v}}{\partial y}, \tilde{T} \to 0 \quad \text{as } y \to \pm\infty.$$

These ensure that the perturbations remain within the mixing layer. It is seen that the scalings introduced to capture the vortices result in the above equations being parabolic in nature. This characteristic is crucial when deciding on a procedure to solve the system. It is possible to impose an initial perturbation at a certain streamwise location, and then integrate the system downstream. The methods employed to solve the disturbance equations are presented in the next section.

2.3. *Numerical methods*

It is worth reiterating that the disturbance equations no longer contain the streamwise diffusion terms. This is because of the disparity in lengthscales in the streamwise, and the normal and spanwise directions. We note that the streamwise pressure gradient of the perturbation is scaled out of the streamwise-momentum equation, which means that the system is parabolic. The disturbance equations can be solved by marching in the downstream direction. First, the normal- and spanwise-momentum equations are combined to eliminate the pressure terms. The conservation of mass equation is then used to eliminate $\tilde{w}$ terms, which leads to a fourth-order equation to solve for $\tilde{v}$, as in the corresponding incompressible problem, Hall (1983) (with an additional second-order equation corresponding to the energy equation). For the sake of brevity we shall not present these equations here; however they are given in Sarkies (1998). It is found to be prudent to exploit the similarity and Howarth–Dorodnitsyn transformations in the numerical scheme. Hall (1983) gives a discussion on the choice of the initial conditions, and also suggests the use of the similarity transformation. In the similarity coordinate the basic-flow calculations can be greatly reduced, and the grid naturally spreads with the mixing layer.

The numerical approach used a standard second-order finite difference scheme in the normal coordinate and a Crank–Nicholson scheme in the downstream coordinate. The finite difference grid in the normal coordinate was stretched in order to decrease computational expense, with outer limits at $Y = \pm 40(X^{1/2})$. The normal coordinate is also elongated or contracted as a result of the Howarth–Dorodnitsyn transformation. This all means that we have coupled tri-diagonal matrices to solve for $\tilde{u}$ and $\tilde{T}$, and a further coupled penta-diagonal matrix for $\tilde{v}$ at each downstream station. We evaluated $\tilde{w}$ using the conservation of mass equation. The procedure followed was to impose an initial perturbation, given later, and then step downstream. At each x-station, we solved for $\tilde{u}$, then $\tilde{T}$ and finally $\tilde{v}$, using the most up-to-date functions available at the time. Then at the same x-station we use a simple iteration on these three equations until $\tilde{u}$ is within a certain tolerance of the previous iterate. The whole procedure is then repeated, stepping downstream. This means that the scheme is fully implicit unlike that used by Wadey (1992), which relieves any limitation on the streamwise step lengths imposed due to numerical stability requirements.

To investigate the stability of the flow we monitor the energy of the disturbance,

quantified by

$$\mathscr{E}(x) = \int_{y=-\infty}^{y=\infty} \tilde{u}^2(x,y)\,\mathrm{d}y = \sqrt{x}\int_{\eta=-\infty}^{\eta=\infty} \bar{T}\tilde{u}^2(x,\eta)\,\mathrm{d}\eta = \sqrt{x}\mathscr{E}_1(x),$$

as the modes progress downstream, Otto *et al.* (1996). Another energy measure we could have used was that employed by Hall (1983) and Wadey (1992). The integrand would then be $\tilde{u}^2 + \tilde{v}^2 + \tilde{w}^2$ rather than $\tilde{u}^2$. This results in a minimal change to the growth rate and the corresponding neutral curves. The growth rate

$$\varsigma(x) = \frac{\mathscr{E}_{1x}}{\mathscr{E}_1} + \frac{1}{2x}$$

is calculated for a particular wavenumber and we are able to determine the neutral point or points, x_n, where $\varsigma(x_n) = 0$.

We study the effect of differing temperature ratios and Mach number. For all cases, curves of neutral stability are obtained by plotting the local wavenumber ($a_x = ax^{1/2}$) against the local Görtler number ($G_x = G\chi x^{3/2}$) where $\varsigma(x) = 0$. It is seen that as we progress downstream (i.e. as x increases) both the local Görtler number and the local wavenumber increase.

The initial conditions used are

$$\tilde{u} = (\mathscr{U} + 2(\eta - \tilde{\eta})^2)\mathrm{e}^{-(\eta-\tilde{\eta})^2}, \quad \tilde{v} = 0, \quad \tilde{T} = \mathscr{M}(\mathscr{T} + 2(\eta - \tilde{\eta})^2)\mathrm{e}^{-(\eta-\tilde{\eta})^2}.$$

This choice is made after consideration of Otto *et al.* (1996). In that paper other initial conditions were tried, including the case when $\tilde{v} \neq 0$ (which represents an initial perturbation with some degree of streamwise vorticity). We note that $\tilde{\eta}$ specifies the initial vertical location of the disturbance. For the majority of this paper we take $\mathscr{U} = \mathscr{T} = 5$, $\tilde{\eta} = -5$ and $\mathscr{M} = 0$; the variation of these parameters (including the use of $\mathscr{M} \neq 0$, depicted in figure 16) only changes the base of the neutral curve. The choice $\tilde{\eta} = -5$ is made so that the disturbances are initially centred within the slower stream; similar results are obtained for other values. Before presenting the solutions to these equations it is instructive to consider the large Görtler number limit of (2) for both order-one and high-wavenumber modes.

3. Far-downstream structure

3.1. *Inviscid Görtler vortices*

In this section we shall give a summary of the results of Owen *et al.* (1997) and extend some of their calculations. We derive a relatively simple condition that can be used to predict which modes a given situation will be prone to. As mentioned in the previous section the local Görtler number and local wavenumber both increase as the modes progress downstream, which is a direct consequence of the natural thickening of the mixing layer. Consequently, we shall discuss the structure of modes in situations with high Görtler numbers. In mixing-layer calculations this divides into two main régimes, and there is a direct matching between these, Otto *et al.* (1996). If one considers modes with order-one scaled wavenumbers in flows characterized by high Görtler numbers, it is found that they develop over short streamwise lengthscales and they are governed by an inviscid equation, Dando & Seddougui (1991). Details of the solution of this equation for this problem are included in Owen *et al.* (1997), incorporating both the conventional and thermal modes. We consider perturbations

of the form

$$(U, G^{1/2}V, G^{1/2}W, GP, T)\exp\left(\int^{x} G^{1/2}(\hat{\beta}(X) + G^{-1/2}\hat{\beta}_1(X) + \cdots)\,\mathrm{d}X + \mathrm{i}az\right),$$

and we combine the resulting equations to obtain

$$\frac{\mathrm{d}^2V}{\mathrm{d}\eta^2} - \frac{2\bar{T}'}{\bar{T}}\frac{\mathrm{d}V}{\mathrm{d}\eta} + \left[-a^2\bar{T}^2 - \frac{\bar{u}''}{\bar{u}} + \frac{2\bar{T}'}{\bar{T}}\frac{\bar{u}'}{\bar{u}} + \frac{a^2\tilde{\chi}}{\beta^2}\left(\frac{\bar{T}\bar{u}'}{\bar{u}} - \frac{\bar{T}'}{2}\right)\right]V = 0, \qquad (3)$$

subject to the boundary conditions $V(\pm\infty) \to 0$. In (3) we have introduced $\beta = \hat{\beta}x^{1/4}/|\chi|^{1/2}$, a is the local wavenumber and $\tilde{\chi} = \mathrm{sgn}(\chi)$. We take $\tilde{\chi} = 1$ to represent concave curvatures and conversely $\tilde{\chi} = -1$ to represent convex curvatures. We can solve the eigenvalue problem (3) numerically (two representative cases are shown in figure 2), and for each of the flows the growth rate β increases monotonically with wavenumber from zero (which is the effectively the left-hand branch of the neutral curve), and eventually asymptotes to a finite value. This is in contrast to a boundary-layer calculation in which the growth rate would tend to infinity with increasing a. Within boundary-layer problems in this limit the modes are driven to the proximity of the solid boundary (at which the underlying streamwise velocity is necessarily zero). Eventually for high enough wavenumbers viscosity will stabilize these modes, Denier *et al.* (1991). In the calculations presented here viscosity will also stabilize the modes although at no point is the underlying flow zero, so we will not encounter the significantly higher growth rates. In figure 3 we show schematics of two configurations, each containing neutral curves and representative growth rates (shown for large Görtler numbers). In figure 3(*a*) we show a neutral curve in which modes grow over extended streamwise distances, Otto *et al.* (1996). Notice that the high-wavenumber limit of the inviscid modes and the low-wavenumber limit of the viscous modes match directly as observed in Taylor problems, Otto & Bassom (1994). In order to determine the growth rate of inviscid modes the numerical solution of the eigenvalue problem (3) is required (as shown in figure 2). Within the intermediate matching régime and for the viscous mode analytical expressions are available to determine the mode growth rates. By considering the intermediate modes we are able to determine the maximum growth rate for modes within high Görtler number situations. If this maximum is negative we find that the neutral curve is closed (as can be seen by extrapolating from figure 3*b*). We shall derive the condition that this maximal growth rate is zero in due course, and we note that this coincides with parameter choices for which the location of the right-hand branch tends to zero. First, we consider the high-wavenumber limit of the inviscid modes, referred to herein as the intermediate matching régime.

It is well known that the highest growth rate is given by consideration of the large-wavenumber limit of the inviscid Görtler problem, see Denier *et al.* (1991) for boundary layers and Otto *et al.* (1996) for mixing layers. We shall thus repeat and extend the analysis presented in Owen *et al.* (1997) which describes the solutions of (3) for $a \gg 1$.

We note that as the wavenumber increases the modes become localized, at η_0 say, and we consider a new variable such that $\eta = \eta_0 + a^{-1/2}\zeta$. We also expand the growth rate β as $\beta_0 + a^{-1/2}\beta_1 \cdots$. At leading order we find that

$$\frac{\beta_0^2}{\tilde{\chi}} = \frac{1}{\bar{T}_0^2}\left(\frac{\bar{T}_0\bar{u}_1}{\bar{u}_0} - \frac{\bar{T}_1}{2}\right) = h(\eta_0), \qquad (4)$$

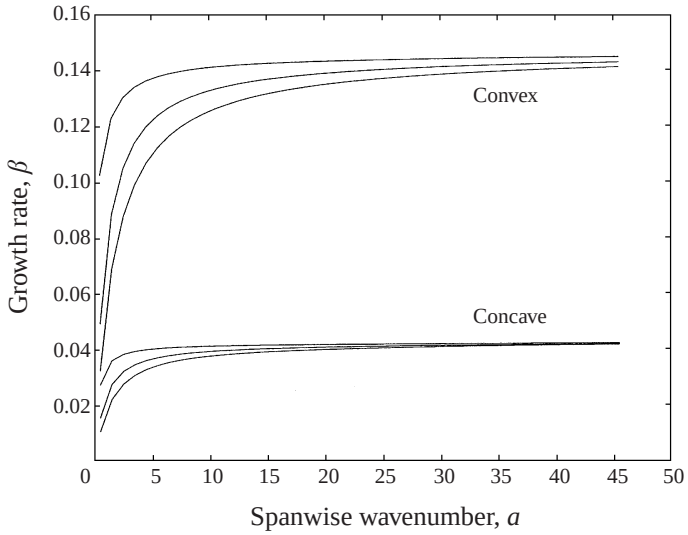

FIGURE 2. Growth rates for the first three modes for concave and convex curvatures for a mixing layer characterized by $\beta_u = 3/2$ and $\beta_t = 5/2$ ($M_\infty = 0$ and $\sigma = 1$). These results were obtained using a global eigenvalue solver. Note that as a increases the growth rate asymptotes monotonically to a finite limit.

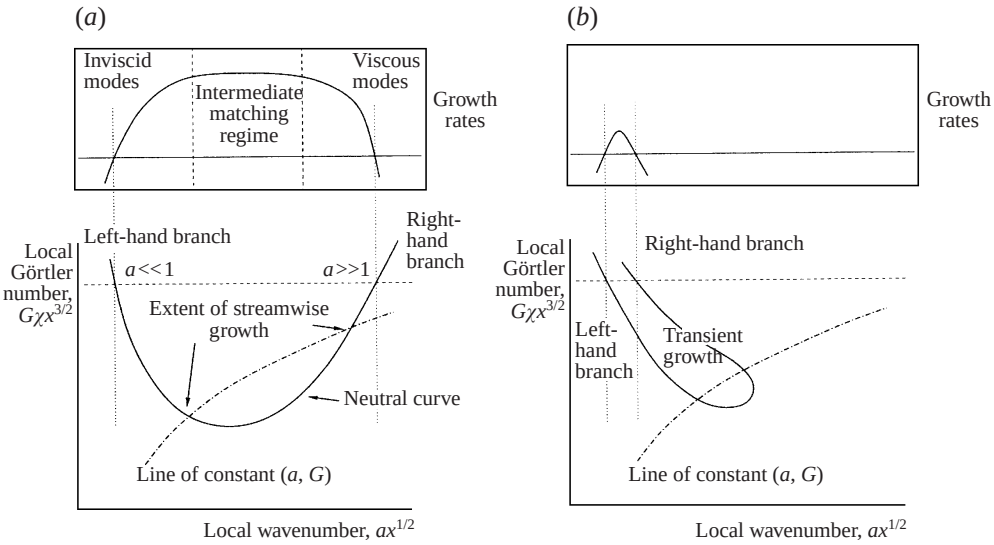

FIGURE 3. Schematic of (*a*) the neutral curve and growth rates for a flow which is unstable to a wide range of wavenumbers and (*b*) a neutral curve for which there is only transient growth. The growth rate is shown as a function of the wavenumber for a large value of the Görtler number represented by the horizontal dashed line.

where the $\bar{.}_j$ denotes the jth term in the Taylor-series expansion at η_0. We note that the expression for β_0^2 can be written as the first term in the Taylor series of

$$\frac{\tilde{\chi}\bar{\rho}^{1/2}}{\bar{u}}\frac{\partial}{\partial\eta}[(\bar{\rho}\bar{u}^2)^{1/2}];$$

thus the condition for instability is unsurprisingly given by Rayleigh's circulation

criterion. The location of the modes is determined as being the point at which the rate of change of circulation achieves an extremum. Accordingly the conditions that we shall derive reflect the occurrence of these points. Note that if the circulation is purely increasing then modes will only occur in the concave case and if it is wholly decreasing then they will only arise in the convex problem. We also note that we can write (3) as a Sturm–Liouville equation, namely

$$\frac{\mathrm{d}}{\mathrm{d}\eta}\left(\frac{1}{\bar{T}^2}\frac{\mathrm{d}V}{\mathrm{d}\eta}\right)+\left[\frac{1}{\beta^2}\left\{\frac{a^2\tilde{\chi}}{\bar{T}^2}\left(\frac{\bar{T}\bar{u}'}{\bar{u}}-\frac{\bar{T}'}{2}\right)\right\}-\left\{a^2+\frac{1}{\bar{u}}\frac{\mathrm{d}}{\mathrm{d}\eta}\left(\frac{\bar{u}'}{\bar{T}^2}\right)\right\}\right]V=0,$$

where we introduce

$$k(\eta)=\frac{1}{\bar{T}^2},\quad g(\eta)=\frac{a^2\tilde{\chi}}{\bar{T}^2}\left(\frac{\bar{T}\bar{u}'}{\bar{u}}-\frac{\bar{T}'}{2}\right),\quad l(\eta)=a^2+\frac{1}{\bar{u}}\frac{\mathrm{d}}{\mathrm{d}\eta}\left(\frac{\bar{u}'}{\bar{T}^2}\right),$$

Synge (1933). We can now infer properties of the eigenvalues of the problem from the structure of the known functions $k(\eta)$, $g(\eta)$ and $l(\eta)$. We notice that provided $l(\eta)\geqslant 0$ for all values of η, $1/\beta^2$ must have the same sign as $g(\eta)$ (notice that this is equal to $a^2\tilde{\chi}h(\eta)$), again provided this has one sign, Ince (1927). This powerful result can be used to show that the findings for $a\gg 1$ will actually be valid provided $l(\eta)\geqslant 0$ (which is obviously so for $a\gg 1$). The condition that $l(\eta)$ is positive for all values of η yields a lower limit for the values of the wavenumber at which one can expect these conclusions to hold. Below this value it is possible that growth may be observed: despite $g(\eta)$ being negative, β^2 may take positive values. For example, for $\beta_t=3$ and $\beta_u=3/2$ this bound is around $a=0.22$. It should be noted that there do not appear to be any unstable modes below this bound; we merely wish to state the possibility of their existence.

At this stage the location of the modes, η_0, remains undetermined; however we note that it will be found in order to maximize β_0^2 (a condition which is found at next order). It is instructive to produce plots of $h(\eta_0)=\beta_0^2/\tilde{\chi}$ for a variety of values of β_t, the free-stream temperature ratio, figure 4. For $\beta_t<1$ there is only one turning point and as β_t decreases the location of the modes tends towards the cooler upper stream, and it may be pertinent to study the small-β_t limit using methods similar to those given in Elliott & Bassom (2000).

As a brief aside we note that as β_t decreases the growth rate increases significantly, see figure 4(*a*). In fact we can show this via analytic consideration of the hyperbolic tangent profile (see the footnote in § 2.1). We note that as $\beta_t\to 0$ the second term in (4) will dominate and hence we consider this part's extremum. The relevant maximum occurs at

$$\eta_0\sim\tanh^{-1}\left\{\frac{\beta_t+1-2\sqrt{1-\beta_t+\beta_t^2}}{\beta_t-1}\right\},\tag{5}$$

which implies that

$$\frac{\beta_0^2}{\tilde{\chi}}\sim\frac{\beta_t^2+1-(1+\beta_t)\sqrt{1-\beta_t+\beta_t^2}}{(\beta_t-1)(\beta_t+1-\sqrt{1-\beta_t+\beta_t^2})^3}.\tag{6}$$

This asymptotes to $(4/27)\beta_t^{-2}$ as $\beta_t\to 0$ (note that we need to use the Howarth–Dorodnitsyn transformation on (4) to get this result). This agrees well with results given in figure 4(*a*) despite the use of the hyperbolic tangent profile ($\beta_t=1/4$ implies $\eta_0\approx 0.94$ and $\beta_0^2/\tilde{\chi}\approx 2.02$). It is easy to show that for any profile $\beta_0=O(\beta_t^{-1})$ as $\beta_t\to 0$ for concave problems ($\tilde{\chi}=1$).

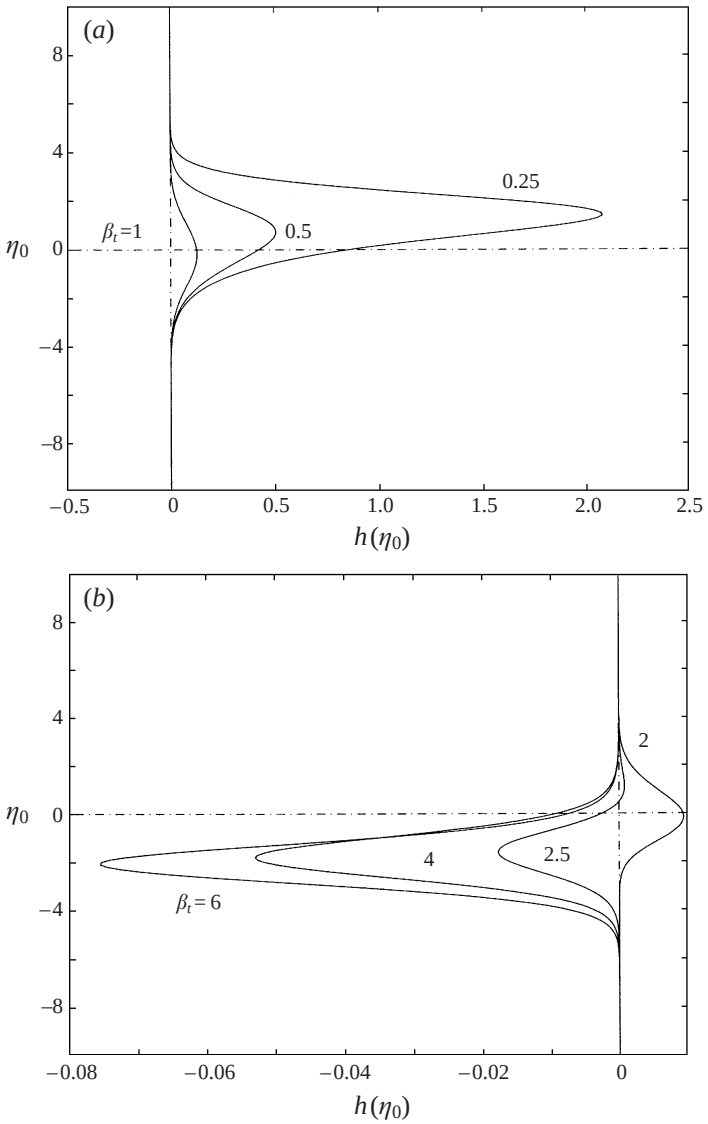

FIGURE 4. (a, b) The variation of the function $h(\eta_0)$ across the mixing layer for a variety of free-stream temperature ratios, $\beta_u = 3/2$, $M_{-\infty} = 0$, $\sigma = 1$ and $\tilde{\chi} = 1$.

At the next order we find that $\beta_1 = 0$ and

$$-\bar{T}_0\bar{T}_1\bar{u}_0\bar{u}_1 + \bar{T}_1^2\bar{u}_0^2 + \bar{T}_0^2\bar{u}_0\bar{u}_2 - \bar{T}_0^2\bar{u}_1^2 - \tfrac{1}{2}\bar{T}_0\bar{T}_2\bar{u}_0^2 = 0,$$

which is the condition that η_0 is at a turning point of $h(\eta_0)$. For $\beta_t > 1$ given in figure 4(b) the choice $\tilde{\chi} = -1$ means that the turning point around $\eta_0 \sim -2$ actually represents unstable modes, although they may have smaller growth rates than the corresponding concave problems. As $\beta_t \to \infty$ we find that the expressions for η_0 and $\beta_0^2/\tilde{\chi}$ again hold, namely (5) and (6) (due to the fact that the same term dominates); however now $\eta_0 \sim \tanh^{-1}(-1 + \beta_t^{-1})$ and $\beta_0^2/\tilde{\chi} \to -4/27 + (2/27)\beta_t^{-1}$.

Finally at third order we find that

$$\frac{\mathrm{d}^2 V_0}{\mathrm{d}\zeta^2} + \left\{ \zeta^2 \left[-(\bar{T}_0 \bar{T}_2 + \bar{T}_1^2) + \frac{\tilde{\chi}}{\beta_0^2} \left(\frac{1}{2\bar{u}_0} [\bar{T}_0 \bar{u}_3 + 2\bar{T}_1 \bar{u}_2 + \bar{T}_2 \bar{u}_1] \right.\right.\right.$$
$$\left.\left.\left. - \frac{\bar{u}_1}{\bar{u}_0^2} [\bar{T}_1 \bar{u}_1 + \bar{T}_0 \bar{u}_2] + \frac{\bar{T}_0 \bar{u}_1}{\bar{u}_0} \left[\frac{\bar{u}_1^2}{\bar{u}_0^2} - \frac{\bar{u}_2}{2} \right] - \frac{\bar{T}_3}{4} \right) \right] - 2\bar{T}_0^2 \frac{\beta_2}{\beta_0} \right\} V_0 = 0, \quad (7)$$

which is given slightly incorrectly in Owen *et al.* (1997). By a simple transformation we find that this equation can be solved in terms of parabolic cylinder functions. As mentioned earlier we note that as the wavenumber increases the viscous terms will eventually come into play, and this then matches directly the corresponding calculation presented later in this section. For a given profile we can determine the likely location of the most unstable modes and their growth rates. It is now possible to make global conclusions concerning the stability of the flow using the function $h(\eta_0)$.

3.2. *Derivation of the parameter ranges for concave and convex configurations*

As mentioned previously it is possible to determine the level of instability by considering the asymptotic limit $a \gg 1$ in the inviscid Görtler problem (which is synonomous with the small-wavenumber limit of the right-hand branch problem discussed in § 3.3). We make the supposition that if modes in this régime are stable then the neutral curve will pinch and it will not be possible to observe sustained streamwise growth, see figure 3. We draw analogies with the inviscid stability or otherwise of a boundary layer. As the Reynolds number tends to infinity the upper and lower branches of the Orr–Sommerfeld curve will remain distinct for an inflectional profile, whereas for an inviscidly stable flow they will eventually merge and the curve will pinch.

We now consider the expression (4) which effectively allows us to determine the growth rate as a function of η_0. At the next order we determine η_0 such that $\partial h/\partial \eta_0$ is zero, which yields modes with growth rates

$$\beta_0 = \sqrt{\tilde{\chi} h(\eta)} \quad \text{evaluated at } \eta = \eta_0 \quad \text{such that } \partial h/\partial \eta = 0 \quad \text{at } \eta = \eta_0.$$

For growing modes we require that β_0 is real and consequently $\tilde{\chi} h(\eta_0)$ must be positive.

In order that the flow is susceptible both to thermal and conventional modes we note that $h(\eta_0)$ must have exactly two turning points (the positive maximum corresponding to the conventional modes and the negative minimum corresponding to the thermal modes). Since the function is zero at plus and minus infinity there must be a further intermediate zero (if the function is to have exactly two turning points). We consider the case of $\sigma = 1$, in which case the temperature is given directly from enthalpy considerations. The zero of h then occurs where

$$\bar{u} = 2 \left(\frac{\beta_u - \beta_t + M_{-\infty}^2 (\gamma - 1) \beta_u (1 - \beta_u)/2}{1 - \beta_t + M_{-\infty}^2 (\gamma - 1)(1 - \beta_u^2)/2} \right).$$

We shall now comment on the location of this zero, and note that unless the corresponding value of $\bar{u}$ lies between 1 and β_u the function h will not have any isolated zeros. This means that it only has one turning point and the flow is only unstable in one of the curvature configurations. In figure 5 we show a schematic of the variation of $\bar{u}|_{h(\eta)=0}$ against β_t for $M_{-\infty} = 0$. For $\beta_t < 1$ there is one branch and this starts for $\beta_t \sim 0$ at $\bar{u} = 2\beta_u$ and increases monotonically: this means that $h(\eta)$ is never zero, and immediately $h(\eta)$ has only one sign (in fact it is positive). For $\beta_t > 1$ the situation

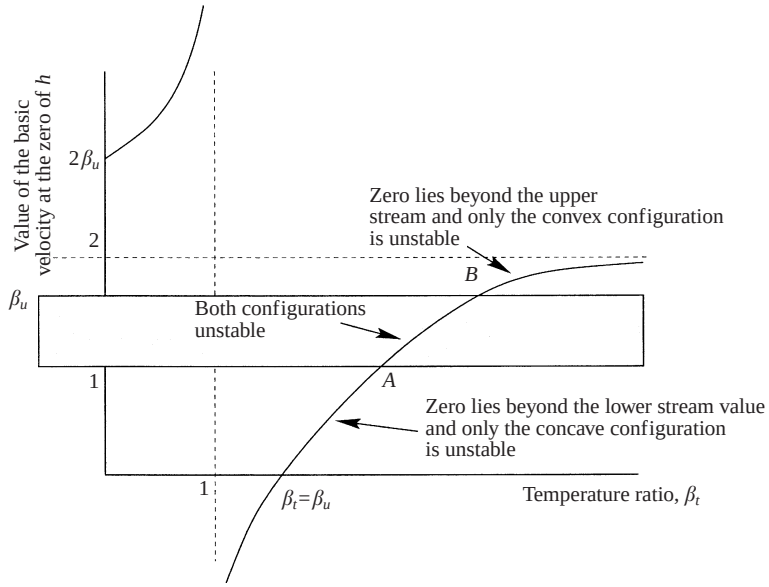

FIGURE 5. The value of $\bar{u}$ at the zero of $h(\eta)$ (for $M_{-\infty} = 0$), as a function of the temperature ratio β_t. The box shows the range $1 < \bar{u} < \beta_u$, which corresponds to $\eta \in [-\infty, \infty]$. Below the shaded box the zero of the function lies beyond $\eta = -\infty$ ($\bar{u} = 1$) and above it corresponds to a zero beyond the upper limit of the mixing layer. The values of β_t at the lower and upper intersection of the curve and the box are $\beta_t^{(A)}$ and $\beta_t^{(B)}$ respectively.

is more complicated. In the interval $1 < \beta_t < \beta_t^{(A)}$ the zero of $h(\eta)$ lies beyond the lower bound of the mixing layer and again $h(\eta)$ has only one sign (implying that only concave configurations are unstable). In the range $\beta_t^{(A)} < \beta_t < \beta_t^{(B)}$, $h(\eta)$ has a zero and hence both configurations are unstable. As β_t increases above $\beta_t^{(B)}$ the zero moves beyond the upper extreme of the mixing layer and again the function $h(\eta)$ has only one sign (which is now negative). As $\beta_t \to \infty$ we note that the curve asymptotes to $\bar{u}|_{h(\eta)=0} = 2$, hence for $\beta_u < 2$ the value of $\beta_t^{(B)}$ is finite, whereas if $\beta_u > 2$ the box would extend vertically beyond the asymptote and the modes in concave configurations would remain unstable for all values of β_t greater than $\beta_t^{(A)}$.

For general Mach numbers the values of β_t at these intersections are

$$\beta_t^{(A)} = 2\beta_u - 1 - \frac{(\gamma - 1)}{2} M_{-\infty}^2 (1 - \beta_u)^2 \tag{8a}$$

and

$$\beta_t^{(B)} = \frac{\beta_u}{2 - \beta_u} \left\{ 1 + \frac{(\gamma - 1)}{2} M_{-\infty}^2 (1 - \beta_u)^2 \right\}. \tag{8b}$$

With the non-dimensionalization used in Owen *et al.* (1997) this yields the cut-off $\beta_t < 1/3$ as shown in figure 19 of that paper and also the condition $\beta_t > 3$ shown here in figure 6 for the existence of the thermal modes, for $M_{-\infty} = 0$. It is worth noting that our argument is independent of the model used for the basic flow (provided that $\partial \bar{u}/\partial y$ does not have any isolated zeros, Zhuang 1999). It is also noted that similar behaviour will occur for Prandtl numbers other than unity. For Prandtl numbers

close to unity (and for $M_{-\infty} = 0$) we expand $\bar{T}$ in powers of $(\sigma - 1)$ to find

$$\bar{T} = 1 + \left(\frac{\beta_t - 1}{\beta_u - 1}\right)(\bar{u} - 1) + (\sigma - 1)\frac{\beta_t - 1}{(\beta_u - 1)^2}\left[(\beta_u - 1)\left[f' \ln f'' + \frac{f^2}{4}\right]_{-\infty}^{\eta} - (\bar{u} - 1)\left[f' \ln f'' + \frac{f^2}{4}\right]_{-\infty}^{\infty}\right] + O((\sigma - 1)^2),$$

where $f(\eta)$ is the solution of (1). The second term requires knowledge of the behaviour of $f(\eta)$ at $\pm\infty$, which is a relatively straightforward exercise. We can show that if $\sigma \neq 1$ then thermal modes arise when $\beta_t > 1$, as shown in figure 6. In order to place an upper bound on the range of β_t for which conventional modes exist further terms need to be taken in the above series.

We now comment on the growth rates for $\beta_u = 3/2$ (figure 4*a*) for both $\tilde{\chi} = 1$ and $\tilde{\chi} = -1$; this quite clearly shows the cut-out (that is the point above which conventional modes do not exist) predicted via the above argument. This cut-out corresponds to $\beta_t^{(B)} = 3 = \beta_u/(2 - \beta_u)$ (for $\sigma = 1$, $M_{-\infty} = 0$ and $\beta_u = 3/2$); for $\beta_t = 5/2$ we see two turning points and for $\beta_t = 4$, $h(\eta_0)$ is purely negative, hence all conventional modes are extinguished (at most we will observe transient growth in § 4 for these parameters, Otto *et al.* 1996).

In summary, via the analysis presented in this section it is possible to determine whether a situation characterized by the values of β_u, β_t and Mach number will be prone to centrifugal modes for concave, convex or both curvatures. We now give the values of β_t for the three cases: for $1 < \beta_u < 2$ we find that

$$\beta_t < 2\beta_u - 1 - \frac{(\gamma - 1)}{2}M_{-\infty}^2(1 - \beta_u)^2 \quad \text{concave unstable,}$$

$$2\beta_u - 1 - \frac{(\gamma - 1)}{2}M_{-\infty}^2(1 - \beta_u)^2 < \beta_t < \frac{\beta_u}{2 - \beta_u}\left\{1 + \frac{(\gamma - 1)}{2}M_{-\infty}^2(1 - \beta_u)^2\right\} \quad \text{both unstable,}$$

$$\frac{\beta_u}{2 - \beta_u}\left\{1 + \frac{(\gamma - 1)}{2}M_{-\infty}^2(1 - \beta_u)^2\right\} < \beta_t \quad \text{convex unstable,} \qquad (9)$$

with similar results for $\beta_u > 2$, although there is no upper bound of β_t for concave situations to be unstable.

It is easy to use a similar analysis to show that no degree of wall cooling will permit sustained growth of centrifugal modes in boundary layers over convex curved plates.

3.3. *Viscous Görtler modes*

The second régime corresponds to points in the neighbourhood of the right-hand branch of the neutral curve, that is where modes will eventually become stable again as they progress downstream. In this régime the viscous terms come into play and the asymptotic location of the right-hand branch can be determined. As mentioned previously there is a direct matching between these two régimes in mixing-layer calculations, unlike the case of Görtler vortices within boundary layers, Denier *et al.*

(1991). On the right-hand branch of the neutral curve $G \sim a^4$ (with $\hat{\lambda} = aG^{1/4}$) and the modes are again localized in a narrow layer of width $a^{-1/2}$ situated at $\bar{\eta}$, which will be determined in due course. Again in this range the growth rate is of order $G^{1/2}$.

We now show the asymptotic analysis for the right-hand branch structure. First, we shall consider the right-hand branch with a view to predicting the kind of behaviour we expect to see via our numerical calculations. We shall proceed with the analysis for non-neutral modes, but will concentrate on neutral disturbances (the growth rate is retained to aid matching with the inviscid calculations). From this we will obtain an expansion of the neutral Görtler number in terms of the neutral wavenumber by setting the growth rate to be zero. We expand the Görtler number as

$$G = a^4(G_0 + a^{-1/2}G_1 + a^{-1}G_2 + \cdots),$$

and consider the solutions within a narrow layer of vortex activity where $\eta = \bar{\eta} + a^{-1/2}\xi$. The vortex quantities are expanded in the form $\tilde{u}(x,\eta) = [\tilde{u}_0(\xi) + a^{-1/2}\tilde{u}_1(\xi) + \cdots]E$, with similar expansions for $a^{-2}\tilde{v}(x,\eta)$, $a^{-3/2}\tilde{w}(x,\eta)$, $a^{-5/2}\tilde{p}(x,\eta)$ and $\tilde{T}(x,\eta)$. Here we have defined E as

$$E = \exp\left[a^2 \int^x (\beta_0 + a^{-1/2}\beta_1 + \cdots)\,\mathrm{d}x\right].$$

We consider steady modes since these are known to be the most unstable within two-dimensional flows, Otto & Denier (1994). We now expand the basic flow as a Taylor-series expansion about $\eta = \bar{\eta}$, to give $\bar{u} = \bar{u}_0(x) + a^{-1/2}\xi\bar{u}_1(x) + \cdots$, with similar expansions for $\bar{v}$ and $\bar{T}$.

These expansions can now be substituted into the disturbance equations (2). We equate like powers of a, and at leading order the expressions obtained from the streamwise-momentum, energy and normal-momentum equations are found to be

$$\left.\begin{aligned} -\bar{T}_0\tilde{u}_0\hat{\lambda}^2 &= \frac{\tilde{v}_0\bar{u}_1}{\bar{T}_0} + \frac{\bar{u}_0\beta_0\tilde{u}_0}{\bar{T}_0}, \quad -\frac{1}{\sigma}\bar{T}_0\tilde{T}_0\hat{\lambda}^2 = \frac{\tilde{v}_0\bar{T}_1}{\bar{T}_0} + \frac{\bar{u}_0\beta_0\tilde{T}_0}{\bar{T}_0}, \\ -\bar{T}_0\tilde{v}_0\hat{\lambda}^2 &= G_0\chi\phi_0\tilde{u}_0 - \frac{G_0\chi}{2}\theta_0\tilde{T}_0 + \frac{\bar{u}_0\beta_0\tilde{v}_0}{\bar{T}_0}, \end{aligned}\right\} \tag{10}$$

where we have introduced the functions $\phi(\eta)$ and $\theta(\eta)$ as $\bar{u}/\bar{T}$ and $(\bar{u}/\bar{T})^2$ respectively (ϕ_j and θ_j are the jth terms in their respective Taylor-series expansions at $\bar{\eta}$).

Note that the equations (10) do not contain any derivatives of the vortex terms and these are combined to obtain a compatibility condition

$$\bar{T}_0\hat{\lambda}^4 = G_0\chi\phi_0\frac{\bar{u}_1}{\bar{T}_0^2} - \frac{G_0\chi}{2}\theta_0\frac{\bar{T}_1\sigma}{\bar{T}_0^2}. \tag{11}$$

This expression yields a condition for the existence of the vortices, and can be used to determine where the instabilities are most likely to occur. We have considered $\beta_0 = 0$ in order to make predictions concerning neutral modes. Alternatively, considering $\hat{\lambda} \to 0$ in (10) requires that β_0 tends to the limit predicted by the large-wavenumber limit of the inviscid problem given in equation (4), hence $\lim_{\hat{\lambda}\to 0}\bar{\eta} = \eta_0$. We now proceed with β_1 and β_2 both set equal to zero.

At next order we have equations which can be combined to obtain an expression purely involving the disturbance quantities $\tilde{v}_0$ and $\tilde{v}_1$. We find that the coefficient of $\tilde{v}_1$ is merely the leading-order compatibility relation (11), which is already satisfied. Considering terms multiplied by $\tilde{v}_0$ we find that $G_1 = 0$; notice that this is only true because we are considering neutral disturbances ($\beta_1 = 0$). The terms multiplying $\tilde{v}_0\xi$

yield

$$\hat{\lambda}^4\bar{T}_1 = G_0\chi\left(\frac{\phi_1\bar{u}_1}{\bar{T}_0^2} - 2\phi_0\frac{\bar{T}_1\bar{u}_1}{\bar{T}_0^3} + \phi_0\frac{\bar{u}_2}{\bar{T}_0^2}\right) - \frac{G_0\chi\sigma}{2}\left(\frac{\theta_1\bar{T}_1}{\bar{T}_0^2} - 2\theta_0\frac{\bar{T}_1^2}{\bar{T}_0^3} + \theta_0\frac{\bar{T}_2}{\bar{T}_0^2}\right). \quad (12)$$

This expression can also be obtained by 'Taylor expanding' the leading-order compatibility relation, and this serves as a check. This condition corresponds to ensuring that when G_0 is obtained from (11) it is at a turning point; that is, we have identified the smallest value of G_0 for this situation at which vortices can arise. Intrinsic to (11) we find a condition which will lead to an expression similar to (9). Hence the conclusions given for the ranges of β_t unsurprisingly also pertain to the right-hand branch régime. This means that a decrease in growth rate is allied to a contraction of the neutral curve, refer to figure 3(*b*).

At third order we find that the viscous terms come into play. The equations can be combined, and making use of the first two compatibility conditions, we find that

$$3\bar{T}_0\frac{\partial^2\tilde{v}_0}{\partial\xi^2} + \xi^2\mathscr{A}\tilde{v}_0 + \frac{G_2}{G_0}\bar{T}_0\hat{\lambda}^2\tilde{v}_0 = 0,$$

the solution of which can be written in terms of parabolic cylinder functions; consequently we require

$$G_2 = \frac{3G_0}{\hat{\lambda}^2}\left(-\frac{4\mathscr{A}}{3\bar{T}_0}\right)^{1/2}(m+\tfrac{1}{2}),$$

where m is zero or a positive integer so that the solutions remain confined within the narrow shear layer. The coefficient $\mathscr{A}$ is given by

$$\begin{aligned}\mathscr{A} = &-\frac{\hat{\lambda}^2\bar{T}_2}{2} + G_0\chi\left[\frac{\phi_2\bar{u}_1}{2\hat{\lambda}^2\bar{T}_0^2} + \left(\phi_1 - \frac{\phi_0\bar{T}_1}{\bar{T}_0}\right)\left(-2\frac{\bar{T}_1\bar{u}_1}{\hat{\lambda}^2\bar{T}_0^3} + \frac{\bar{u}_2}{\hat{\lambda}^2\bar{T}_0^2}\right)\right.\\
&\left.-\frac{\phi_0\bar{T}_2}{2\bar{T}_0^3}\frac{\bar{u}_1}{\hat{\lambda}^2} + \frac{\phi_0}{2\hat{\lambda}^2\bar{T}_0}\left(\frac{\bar{u}_3}{\bar{T}_0} - 2\frac{\bar{u}_2\bar{T}_1}{\bar{T}_0^2} - \frac{\bar{u}_1\bar{T}_2}{\bar{T}_0^2} + 2\frac{\bar{u}_1\bar{T}_1^2}{\bar{T}_0^3}\right)\right]\\
&-\frac{G_0\chi\sigma}{2}\left[\frac{\bar{T}_1\theta_2}{2\hat{\lambda}^2\bar{T}_0^2} + \left(\theta_1 - \frac{\theta_0\bar{T}_1}{\bar{T}_0}\right)\left(-2\frac{\bar{T}_1^2}{\hat{\lambda}^2\bar{T}_0^3} + \frac{\bar{T}_2}{\hat{\lambda}^2\bar{T}_0^2}\right)\right.\\
&\left.-\frac{\bar{T}_1\bar{T}_2\theta_0}{2\hat{\lambda}^2\bar{T}_0^3} + \frac{\theta_0}{2\hat{\lambda}^2\bar{T}_0}\left(\frac{\bar{T}_3}{\bar{T}_0} - 3\frac{\bar{T}_1\bar{T}_2}{\bar{T}_0^2} + 2\frac{\bar{T}_1^3}{\bar{T}_0^3}\right)\right].\end{aligned}$$

It is noted that $\mathscr{A}$ is the local expansion of the second derivative of (11) with respect to η. This quantity is taken to be a maximum for a positive curvature (concave) and a minimum for negative curvature (convex). This implies that $\mathscr{A}$ is always negative with the requisite choice of the sign of χ (that is $\tilde{\chi}$).

Defining the local Görtler number and wavenumber as in § 2.3 we have the first two terms in the local Görtler number expansion as

$$G_x = a_x^4 G_0\left[1 + a_x^{-1}\frac{3}{\hat{\lambda}^2}\left(-\frac{4\mathscr{A}}{3\bar{T}_0}\right)^{1/2}(m+\tfrac{1}{2}) + \cdots\right], \quad (13)$$

which is the compressible analogue of the expression given in Hall (1983). Hall notes that in order to obtain the next term in the expansion one is required to incorporate non-parallel terms.

The first two conditions, namely (11) and (12), can be used to determine the Görtler number G_0 and the mode location $\bar{\eta}$. These conditions have been used in Wadey (1991) and Owen *et al.* (1998) to predict the onset of nonlinear vortex structures. In the asymptote (13) we take $m = 0$, which corresponds to the first mode. It is noted that G_x increases as m increases, implying that the higher modes are more stable.

The location of the right-hand branch is a good indication of the level of instability: as the right-hand branch moves to the right more wavenumbers are unstable for greater distances downstream. In contrast, for some cases the right-hand branch moves so far to the left that the neutral curve pinches. In these cases we would only expect to observe transient growth, see for instance the modes found in Otto *et al.* (1996) for convex curved mixing layers, see figure 3(*b*). It is well known that on the right-hand branch of the neutral curve $G \sim a^4$ (for $\chi \sim \sqrt{x}$), where the value of $\hat{\lambda}$ determines the multiplicative constant. In figure 6 we show how the value of $\hat{\lambda}$ varies as β_t changes for neutral modes. The curves shown are for $\beta_u = 3/2$ and $M_{-\infty} = 0$ (similar results are obtained for other values). For $\tilde{\chi} = -1$, which corresponds to convex curvature, as the relative temperature of the faster stream decreases the location of the right-hand branch moves to the left (i.e. $\hat{\lambda} \to 0$) until the neutral curve eventually pinches (at $\beta_t = 2 = 2\beta_u - 1$ for $\sigma = 1$) as predicted via (9). The location of the right-hand branch for the compressible counterparts of the modes found in Otto *et al.* (1996) is labelled 'conventional modes'. If $\tilde{\chi} = 1$ we observe conventional modes but only for $\beta_t < 3$ (for $\sigma = 1$). It is seen that for a Prandtl number of 0.72 even though the bounds of the inequality are modified, the conclusions remain largely unchanged. As β_t decreases here, that is the faster stream decreases in temperature, more modes become unstable. We show the effect of changing Mach number on the location of the right-hand branch in figure 7 for conventional modes. The curves show that as the Mach number increases the right-hand branch moves slightly to the left (shown as a decrease in the neutral wavenumber). It can be seen in this and the previous figure that as β_t decreases for the conventional modes the right-hand branch of the neutral curve moves to the right quite dramatically, refer to figure 11. It appears that these modes will operate over a wider range of wavenumbers and be more unstable than their counterparts in uncooled situations.

4. Results from the numerical solutions of equations (2)

We now discuss the results obtained from the numerical calculations for different parameter choices, and make comparisons with the right-hand-branch asymptotic theory presented in the previous section. In this section we shall mainly be concerned with the shape of the neutral curves; however we note that it is also necessary to consider the growth rates of the modes. Interestingly, via the analysis of the previous section and the direct calculations we find that an enlarging of the neutral curves is accompanied by an increase in growth rate. Hence modes are more unstable as well as persisting over a wider parameter régime, and vice versa for contracting neutral curves.

All perturbations are imposed at $\bar{x} = 20$, unless otherwise stated. This is a position where the basic flow is assumed to be fully developed. In Hall (1983), the neutral curves shared the same right-hand branch for different values of $\bar{x}$, but with distinct left-hand branches. In the mixing-layer problem, none of the neutral curves actually cross each other, but a neutral curve will lie inside one that has a smaller value of

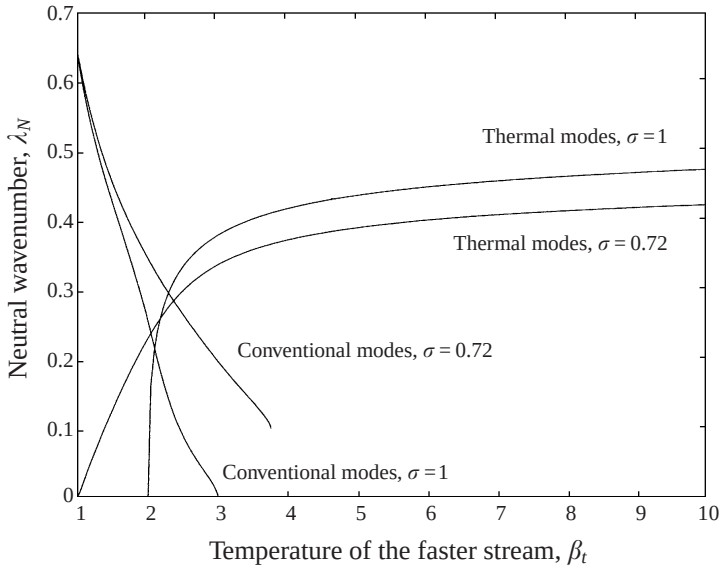

FIGURE 6. The asymptotic location of the right-hand branch as a function of β_t with the cut-outs as predicted using (9) for the maximum growth rate (with $M_{-\infty} = 0$ and $\beta_u = 3/2$). Note that the tending to zero of the neutral wavenumber corresponds to a pinching of the neutral curve, whereas the fact that it increases as $\beta_t \to 0$ for conventional modes describes the spreading of the curve. (Note that these modes were shown to have asymptotically higher growth rates.)

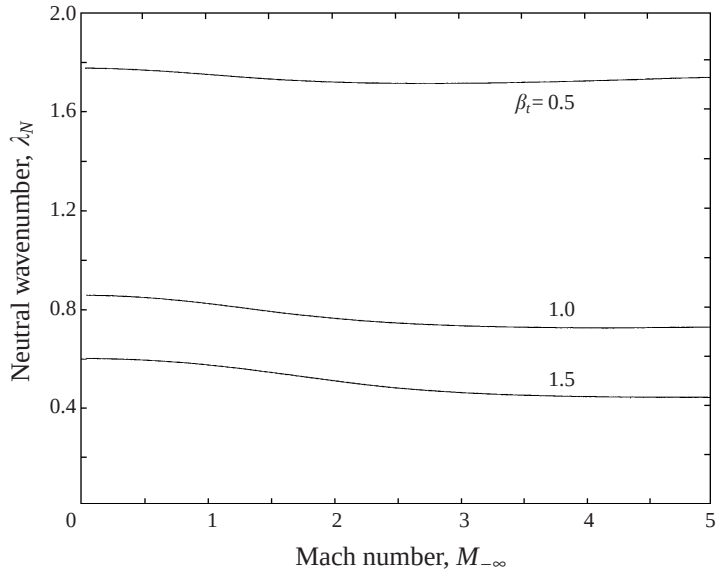

FIGURE 7. The asymptotic location of the right-hand branch as a function of Mach number, $\sigma = 0.72$, $\beta_u = 3/2$, $\tilde{\chi} = 1$.

$\bar{x}$. This can be seen for the incompressible problem in figure 8. We choose $\bar{x} = 20$ from consideration of Otto *et al.* (1996), so that the validity of our results can be checked in the incompressible limit, $M_{-\infty} = 0$. We also have taken the curvature to be $\sqrt{x/\bar{x}}$ in most calculations, although in figure 9 we plot neutral curves for two

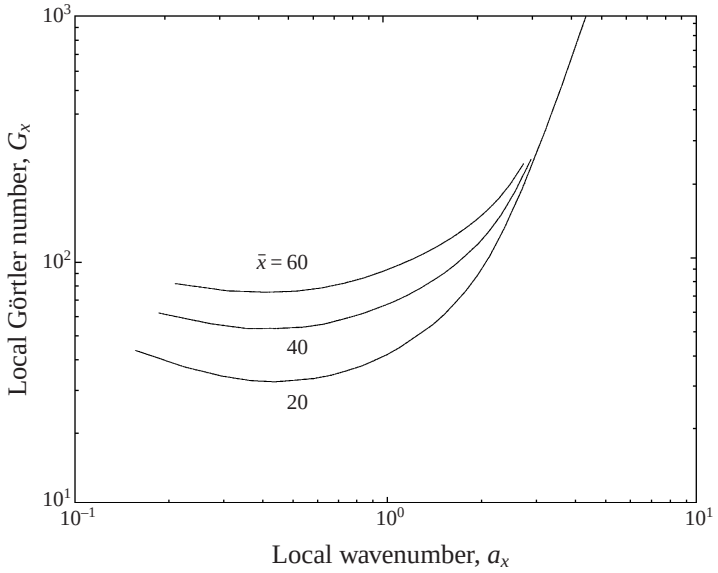

FIGURE 8. Neutral curves for $\bar{x} = 20$, 40, 60 with $G = 1/20$, $M_{-\infty} = 0$, $\beta_u = 2$, $\beta_t = 1$.

different curvatures. It can be seen that for a constant curvature of $\chi = 1$, the base of the neutral curve is lower than for a curvature of $\chi = \sqrt{x/\bar{x}}$. Also the right-hand branches cross for these two curvatures. The effect of changing β_u was shown in Otto *et al.* (1996) to be that an increase renders the flow more unstable. We use a Görtler number of $1/20$; this is not particularly significant but is chosen so that there is a reasonable streamwise distance until the modes start to grow. Increasing and decreasing the Görtler number has the simple effect of enhancing or inhibiting the instability mechanism, both in terms of growth rate and distance before they start to grow.

We now turn our attention to the effect of the Mach number on the stability of the flow. In § 3.2 we see that, via (11) and (12), we can predict that an increase in $M_{-\infty}$ brings about a decrease of instability, that is a smaller range of wavenumbers is unstable. This can be seen in figure 7. Interpreting these results, we expect that the right-hand branch of the neutral curve should move subtly to the left with an increase in Mach number. In figure 10 we give neutral curves corresponding to conventional Görtler modes where this result is found. The results suggest that in this case, the effect of compressibility is to stabilize the flow. Also plotted on the figure is the two-term asymptote calculated using equation (13), for the case $M_{-\infty} = 2/5$. The agreement for this case is good, as has been found for the other cases, although for clarity these asymptotes have been omitted.

Next, we consider the effect of changing β_t, the temperature of the upper faster stream (recall that in this study, the lower stream has non-dimensional velocity and temperature equal to unity). Again we can predict the location of the right-hand branch using the asymptotic methods presented in § 3. For $\tilde{\chi} = 1$, that is the centreline curves towards the faster stream, we find that a decrease in β_t increases the range of wavenumbers for which growing modes can be found. In figure 11 we show four neutral curves; the most unstable case shown corresponds to $\beta_t = 1/2$. For smaller values of β_t the right-hand branch would appear even further to the right. It seems that only a slight change in β_t will dramatically change the stability of the flow. Again

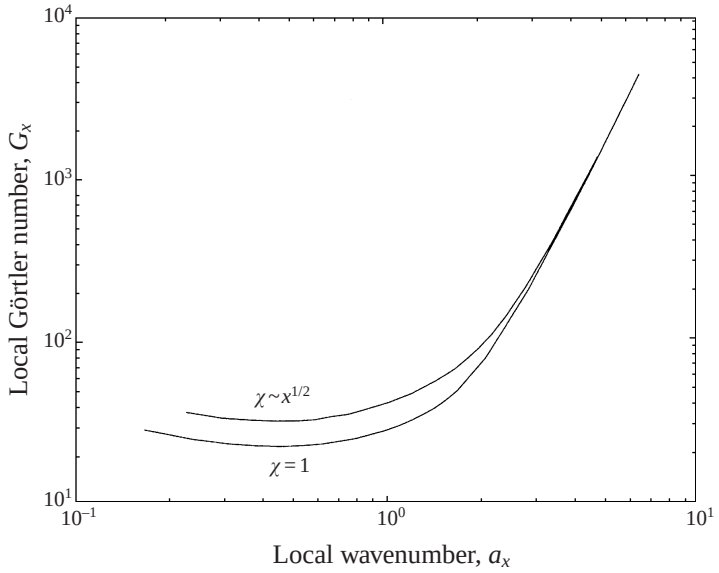

FIGURE 9. Neutral curves for $\chi = 1$ and $\chi = (x/\bar{x})^{1/2}$ with $G = 1/20$, $M_{-\infty} = 0.4$, $\beta_u = 2$, $\beta_t = 1$.

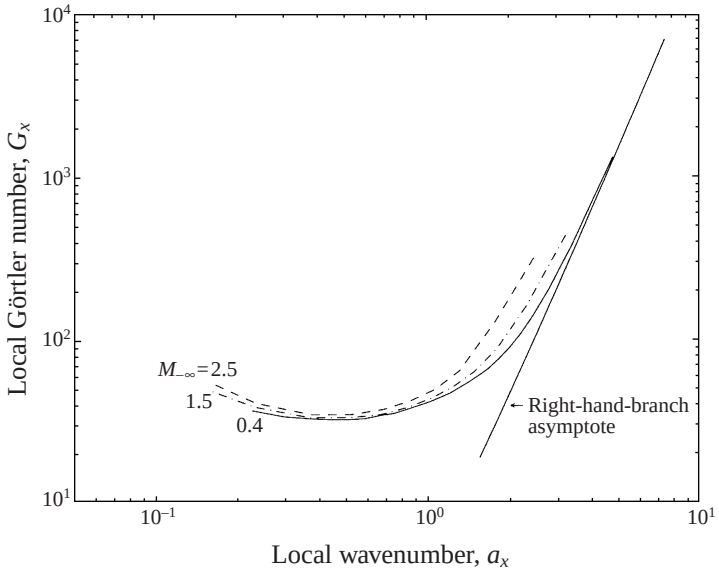

FIGURE 10. Neutral curves for $G = 1/20$ for different values of the Mach number with $\beta_t = 1$.

equation (13) has been used to calculate an asymptote for the case $\beta_t = 1/2$ and reasonable agreement is found. It is expected that higher terms in the expansion will yield closer results. The aim here is to ascertain that the numerical results are close to the analytical findings, and this is found to be the case. It is also noted that at the next order in the asymptotic approximation, non-parallel flow effects start to enter the solution.

We now turn our attention to modes within mixing layers where the curvature is away from the faster stream ($\tilde{\chi} = -1$). From figure 6 we see that unless β_t is

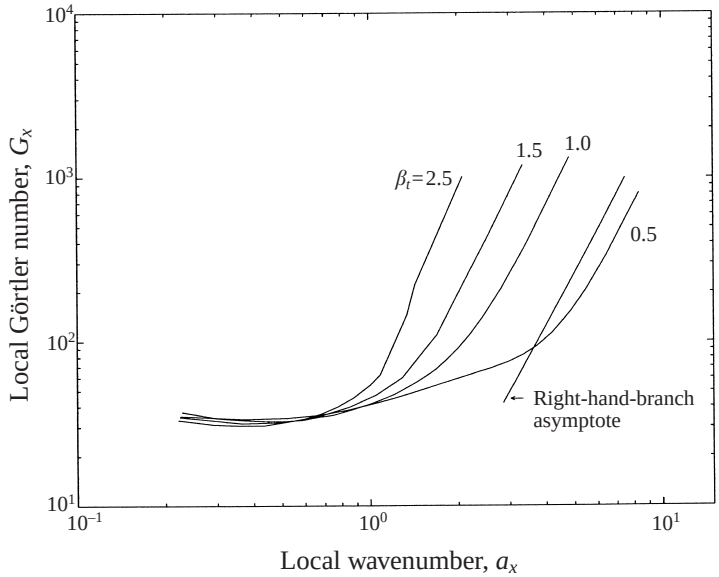

FIGURE 11. Neutral curves for $G = 1/20$, showing a variety of values of temperature ratios with $M_{-\infty} = 2/5$ and $\beta_u = 2$.

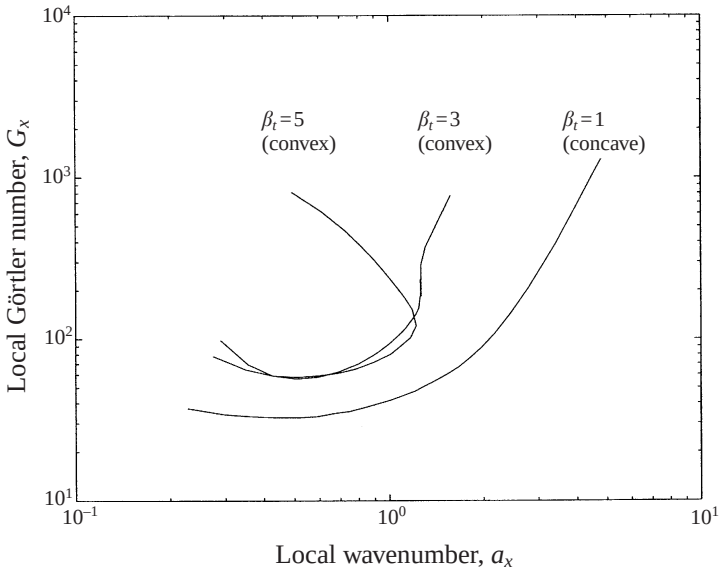

FIGURE 12. Neutral curves for $G = 1/20$ with $\tilde{\chi} = -1$, showing a variety of values of temperature ratio with $M_{-\infty} = 2/5$ and $\beta_u = 2$ ($\sigma = 0.72$) (the neutral curve for $\beta_t = 1$ and $\tilde{\chi} = 1$ is included for comparison).

greater than 3 the majority of modes will be stable downstream (for $\sigma = 1$, $\beta_u = 3/2$, $M_{-\infty} = 0$). Neutral curves for two values of β_t are shown in figure 12 (with the $G = 1/20$, $\beta_t = 1$ case included for comparison). For $\beta_t = 3$ the right-hand branch has been pushed to the left so that there is only transient growth, cf. figure 6. Even for $\beta_t = 5$ the right-hand branch is still not very far to the right. These modes have

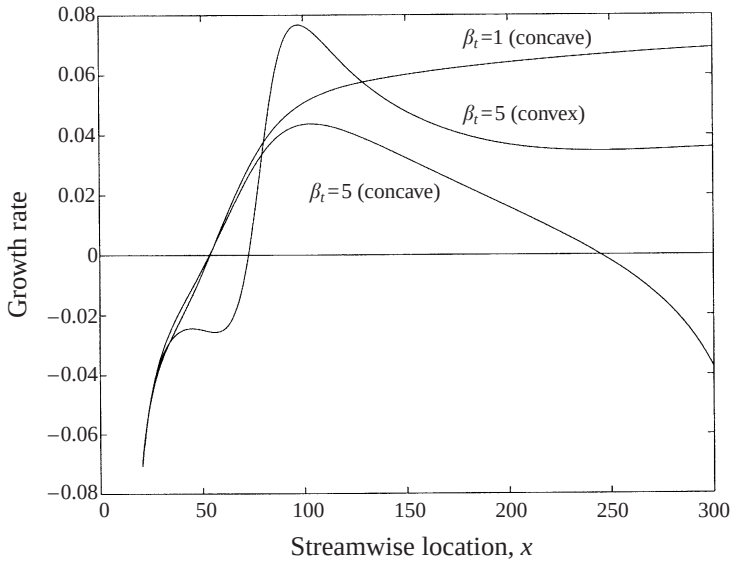

FIGURE 13. Growth rates shown for a variety of situations, $M_{-\infty} = 2/5$, $\beta_u = 2$, $a = 1/20$ and $G = 1/20$.

no counterpart in the incompressible problem, and again it is seen that the disparity in temperatures between the two streams plays an important rôle in determining the stability of the centrifugal modes.

In figure 13 we show the growth rates for $a = 1/20$ for a variety of cases. Note that the two curves corresponding to $\beta_t = 5$ show very different behaviour: far downstream the modes become stable where the layer curves into the faster stream ($\tilde{\chi} = 1$), which is not true for curvature in the other sense ($\tilde{\chi} = -1$). The growth rates in figure 14 are shown for an optimal wavenumber for the flow situation; the optimal wavenumber is defined by the mode with the maximum sustained growth rate. It is seen that as β_t decreases, the maximum growth rate increases, as suggested by the analysis given in § 3.

We now recall that for $\beta_u < 2$ there will be a finite range of β_t for which conventional modes operate. From figure 15, with $\beta_u = 3/2$ we notice that for $\beta_t = 2$ the neutral curve has an open right-hand branch. For the case $\beta_t = 4$ we see that the right-hand branch is folding over, as was seen for the thermal modes for $\sigma = 1$ (figure 12); this corresponds to only transient growth. In such cases, the mode growth rate becomes positive only for very short streamwise distances. It is then seen that the inequalities presented in the previous section allow us to glean information as to whether a flow will support centrifugal instabilities. In figure 15 we also include neutral curves for $\sigma = 0.72$; as suggested by figure 6 these lie further to the right than those with unity Prandtl numbers. Notice in particular for $\beta_t = 4$ the contrast between $\sigma = 1$ and $\sigma = 0.72$, cf. figure 6.

In figure 16 we see the effect of changing the initial conditions. The lower curve uses the initial conditions given previously with $\mathscr{M} = 0$, that is with no initial temperature perturbation, and the upper curve uses the initial conditions with $\mathscr{M} = 1$. The cases in between are for $\mathscr{M} = 1/2$, $\mathscr{M} = 3/4$ and $\mathscr{M} = 9/10$. For the case $\mathscr{M} = 1$, the neutral curve doubles back on itself. It asymptotes to the same right-hand branch as the $\mathscr{M} = 0$ case, as expected. It is also seen that as the value of $\mathscr{M}$ is increased, the 'kink' becomes more pronounced. This effect is largely a transient due to the initial conditions.

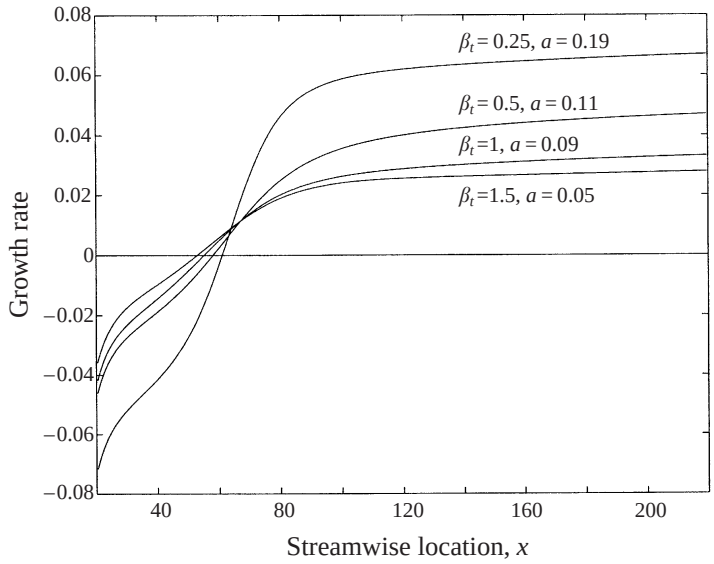

FIGURE 14. Optimal growth rates shown for a variety of situations, $M_{-\infty} = 2/5$, $\beta_u = 2$, $G = 1/20$. Note the increase in growth rate with decrease in β_t as predicted in § 3.1.

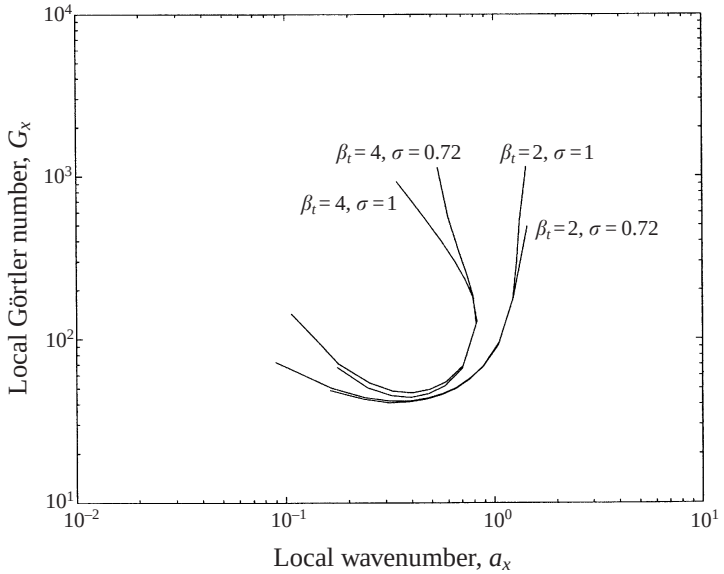

FIGURE 15. Neutral curves for $\beta_u = 3/2$, $M_{-\infty} = 0$, $G = 1/20$.

5. Conclusions

In this paper it has been shown that centrifugal instabilities can exist in curved compressible mixing layers. The work here agrees in the incompressible limit with Otto *et al.* (1996). Effects such as change in curvature or ratio of the free-stream velocities are largely found to have similar ramifications when the flow is compressible. The compressibility of the flow also introduces parameters that have been seen to alter the flow's susceptibility to centrifugal instabilities. In the main we require the slower

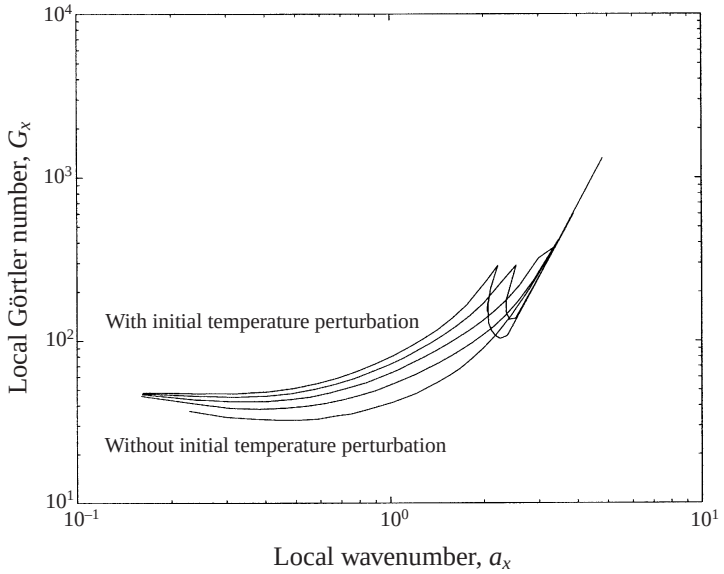

FIGURE 16. Neutral curves for $\mathscr{M} = 0, 1/2, 3/4, 9/10, 1$(upper curve), for $M_{-\infty} = 2/5$, $\beta_t = 1$ and $G = 1/20$.

stream to curve into the faster stream to generate streamwise vorticity; however if the faster stream curves into a cooler slower stream then centrifugal instabilities are also likely to be observed. These modes were first described in Owen *et al.* (1997) and here we have obtained them using a full numerical calculation. We have also been able to determine a measure of the ranges of parameters over which one would expect to observe them. This range was predicted using an asymptotic limit of the governing equations and was seen to accurately determine what was observed via our direct calculations. This method of predicting ranges for which one would expect to observe sustained growth of this class of modes also allows us to make some comments concerning the effect of other parameters. In (9) we give ranges of free-stream temperature ratios for which both thermal and conventional modes persist; from this we can infer that as the Mach number of the lower stream increases, the value of the temperature ratio at which thermal modes occur decreases thus rendering the situation more unstable to these modes. In fact an increase in Mach number increases the maximum growth rate of the thermal modes, but only very slightly. In the main however, the variation of the Mach number is seen to have a similar effect to that in most other compressible flows, that is an increase in Mach number tends to produce a stabilizing influence, Wadey (1992). Another result we note concerning the variation of the free-stream temperature ratio, β_t, is that for the concave case ($\tilde{\chi} = 1$) the growth rate is of order β_t^{-1} as the upper stream decreases in temperature (which is significant). For the convex case ($\tilde{\chi} = -1$) as the temperature of the upper stream increases the growth rate tends to a constant. Both these results are largely independent of the free-stream velocity ratios. It is also worth noting the significant rôle of the Prandtl number, for instance in determining the minimum temperature ratio at which the thermal modes are likely to arise. In problems with different Prandtl numbers the ranges at which these modes operate are likely to be significantly modified.

It has been shown that conventional Görtler modes in a situation with a cooler faster stream are more unstable than their counterparts in uncooled situations, and persist over a larger range of wavenumbers. Again using the inequalities (9) we can show that for free-stream speed ratios less than two there is an upper bound of free-stream temperature ratios for which conventional modes may be sustained. The numerical results have been checked via an asymptotic analysis, which predicts the location of the right-hand branch of the neutral curve and the variation of the maximum growth rate.

In summary we can use the expression (4) to draw conclusions on the fate of centrifugal modes. If the curvature is concave ($\tilde{\chi} = 1$) then we require that the combination ($T_0 u_1 - T_1 u_0/2$) is positive. The effect of a larger velocity gradient will be diminished as the temperature gradient becomes large and positive. Alternatively, for $\beta_t < 1$ the temperature gradient will be negative, and the velocity and temperature gradients will both augment the growth rate in a constructive way. For the convex case we require that the temperature gradient is large and positive ($\beta_t > 1$), but as the magnitude of the velocity gradient increases these modes will gradually be extinguished.

Other results such as a change in curvature of the layer are seen to agree with the findings of Otto *et al.* (1996). A change in initial streamwise location of the disturbance was also investigated, and it was seen that the base of the neutral curve was altered although the right-hand branches merged as expected. If there is an initial temperature perturbation then there is a kink in the neutral curve for the case considered here, refer to figure 16.

Perhaps the most interesting point raised by this work is the possible effect of Görtler vortices on the intrinsic inviscid modes; Owen *et al.* (1998). Since the underlying flow now varies with y and z we would need to solve a two-dimensional eigenproblem, as derived in Hall & Smith (1991). In Hu *et al.* (1994) and Liou (1994) it is noted that the presence of curvature has a minimal effect directly on the inflectional modes. However, in Otto (1995) it was shown that as the amplitude of the Görtler vortices in pressure-gradient-driven flows increased, the intrinsic Rayleigh modes were further destabilized. In Seddougui & Otto (1995) and Owen *et al.* (1998) it has been observed that for nonlinear vortices in the neighbourhood of the right-hand branch, the presence of the vortices serves to reduce the growth rates of the inherent inviscid instabilities for the case of a slower flow curving into a faster one. However, for the thermal modes Owen *et al.* (1998) observed a destabilization of the inviscid modes, as also observed in boundary layers in Otto (1995). The solution of the incompressible version of the two-dimensional Rayleigh equation was discussed in Hall & Horseman (1991) and Otto & Denier (1993) for Görtler vortices within boundary layers. The solution of the corresponding mixing-layer problem is presented in Otto *et al.* (2000).

Other work that this study might lead to includes the nonlinear evolution of the modes, in the fashion of Hall (1988). This will allow us to more accurately predict the fate of Görtler vortices and inviscid instabilities within curved mixing layers, and consequently determine their influence on mixing properties.

The first author would like to thank EPSRC for providing funding during the course of this work. We would also like to acknowledge Professor Scorer for pointing out the occurrence of these instabilities in meteorological systems. The authors would also like to thank Dr Jim Denier for his comments concerning an earlier draft of this work, and the referees for their helpful comments.

REFERENCES

Bell, J. H. & Mehta, R. D. 1990 Development of a two-stream mixing layer within tripped and untripped boundary layers. *AIAA J.* **28**, 2034–2042.

Blackaby, N. D. 1991 On viscous, inviscid and centrifugal instability mechanisms in compressible boundary layers, including nonlinear vortex/wave interaction and the effects of large Mach number on transition. PhD thesis, University of London.

Dando, A. H. & Seddougui, S. O. 1991 The compressible Görtler problem in two-dimensional boundary layers. *IMA J. Appl. Maths* **51**, 27–67.

Denier, J. P., Hall, P. & Seddougui, S. O. 1991 On the receptivity problem for Görtler vortices: vortex motions induced by wall roughness. *Phil. Trans. R. Soc. Lond.* A **335**, 51–85.

Elliott, J. W. & Bassom, A. P. 2000 The effect of wall cooling on compressible Görtler vortices. *Euro. J. Mech.* B/*Fluids* **19**, 37–68.

Floryan, J. M. & Saric, W. S. 1979 Stability of Görtler vortices in boundary layers. *AIAA Paper* 79-1497, pp. 316–324.

Görtler, H. 1940 Über eine dreidimensionale instabilität laminarer Grenzschichten an Konkaven wänden. *Ges. D. Wiss. Göttingen* 1.

Gutmark, E. J., Schadow, K. C. & Yu, K. H. 1995 Mixing enhancement in supersonic free shear flows. *Ann. Rev. Fluid Mech.* **27**, 375–417.

Hall, P. 1982 Taylor-Görtler vortices in fully developed or growing boundary-layer flows: linear theory. *J. Fluid Mech.* **24**, 475–494.

Hall, P. 1983 The linear development of Görtler vortices in growing boundary layers. *J. Fluid Mech.* **130**, 41–58.

Hall, P. 1988 The nonlinear development of Görtler vortices in growing boundary layers. *J. Fluid Mech.* **193**, 243–266.

Hall, P. & Horseman, N. J. 1991 The linear inviscid secondary instability of longitudinal vortex structures in boundary layers. *J. Fluid Mech.* **232**, 357–375.

Hall, P. & Smith, F. T. 1991 On strongly nonlinear vortex/wave interactions in boundary layer transition. *J. Fluid Mech.* **227**, 641–666.

Hu, F. Q., Otto, S. R. & Jackson, T. L. 1994 On the stability of a curved mixing layer. In *Proc. ICASE workshop on Transition, Turbulence and Combustion* (ed. M. Y. Hussaini, T. B. Gatski & T. L. Jackson), pp. 107–116. Kluwer.

Ince, E. L. 1927 *Ordinary Differential Equations.* London: Longmans Green.

Karasso, P. S. & Mungal, M. G. 1997 Mixing and reaction in curved liquid shear layers. *J. Fluid Mech.* **334**, 381–409.

Klemp, J. B. & Acrivos, A. 1972 A note on the mixing of two uniform parallel semi-infinite streams. *J. Fluid Mech.* **55**, 25–30.

Liou, W. W. 1994 Linear instability of curved free shear layers. *Phys. Fluids* **6**, 541–549.

Lock, R. C. 1951 The velocity distribution in the laminar boundary layer between parallel streams. *Q. J. Mech.* **4**, 42–57.

Mack, L. 1984 Boundary-layer linear stability theory. *Tech. Rep.* 709. AGARD.

Michalke, A. 1964 On the inviscid instability of the hyperbolic tangent velocity profile. *J. Fluid Mech.* **19**, 543–556.

Otto, S. R. 1995 On the secondary instability of Görtler vortices in Three-Dimensional Boundary Layers. In *Proc. IUTAM Symp. on Nonlinear Instability and Transition in Three-Dimensional Boundary Layers* (ed. P. W. Duck & P. Hall), pp. 85–94. Kluwer.

Otto, S. R. & Bassom, A. P. 1994 The effect of crossflow on Taylor vortices. *Q. J. Mech. Appl. Maths* **47**, 323–339.

Otto, S. R. & Denier, J. P. 1993 On the secondary instability of the most dangerous Görtler vortex. In *IUTAM Symp. on Nonlinear Instability of Nonparallel flows* (ed. S. P. Lin, W. R. C. Phillips & D. T. Valentine), pp. 290–299. Springer.

Otto, S. R. & Denier, J. P. 1994 On the effect of crossflow on Görtler vortices. In *Proc. ICASE workshop on Transition, Turbulence and Combustion* (ed. M. Y. Hussaini, T. B. Gatski & T. L. Jackson), pp. 215–224. Kluwer.

Otto, S. R., Jackson, T. L. & Hu, F. Q. 1996 On the spatial evolution of centrifugal instabilities within curved incompressible mixing layers. *J. Fluid Mech.* **315**, 85–103.

Otto, S. R., Sarkies, J. M. & Denier, J. P. 2000 On the effect of Görtler vortices on Kelvin-Helmholtz modes. (In preparation.)

Otto, S. R., Stott, J. A. K. & Denier, J. P. 1999 On the role of buoyancy in determining the stability of curved mixing layers. *Phys. Fluids* **11**, 1495–1501.

Owen, D. J., Seddougui, S. O. & Otto, S. R. 1997 The linear evolution of centrifugal instabilities in curved, compressible mixing layers. *Phys. Fluids* **9**, 2506–2518.

Owen, D. J., Seddougui, S. O. & Otto, S. R. 1998 The nonlinear evolution of centrifugal instabilities in curved, compressible mixing layers. *Phys. Fluids* **10**, 2080–2090.

Plesniak, M. W., Mehta, R. D. & Johnson, J. P. 1994 Curved two-stream turbulent mixing layers: three-dimensional structure and streamwise evolution. *J. Fluid Mech.* **270**, 1–50.

Plesniak, M. W., Mehta, R. D. & Johnson, J. P. 1996 Curved two-stream turbulent mixing layers revisited. *Expl Therm. Fluid Sci.* **13**, 190–205.

Rasmussen, M. 1994 *Hypersonic Flow*. John Wiley & Sons.

Sarkies, J. M. 1998 On the stability of compressible boundary layers. PhD thesis, The University of Birmingham.

Sarkies, J. M. & Otto, S. R. 1998 On the downstream evolution of centrifugal instabilities in curved compressible mixing layers: linear problem. In *Proceedings of EMAC98, Adelaide. IAustE* (ed. E. O. Tuck & J. A. K. Stott), pp. 451–454.

Sarkies, J. M. & Otto, S. R. 1999 On the stability of a compressible Rayleigh layer. *Theor. Comput. Fluid Dyn.* (submitted).

Scorer, R. S. 1997 *Dynamics of Meteorology and Climate*. Wiley.

Scorer, R. S. & Wilson, S. D. R. 1963 Secondary stability in steady gravity waves. *Q. J. R. Mete. Soc.* **89**, 532–539.

Seddougui, S. O. & Otto, S. R. 1995 On the nonlinear evolution of Görtler vortices in curved mixing layers. In *Proc. IUTAM Symp. on Nonlinear Instability and Transition in Three-Dimensional Boundary Layers* (ed. P. W. Duck & P. Hall), pp. 95–104. Kluwer.

Stewartson, K. 1964 *The Theory of Laminar Boundary Layers in Compressible Fluids*. Oxford University Press.

Stott, J. A. K. & Denier, J. P. 1998 The stability of boundary layers on curved heated plates. *J. Aust. Maths* B. (submitted).

Swearingen, J. D. & Blackwelder, R. F. 1987 The growth and breakdown of streamwise vortices in the presence of a wall. *J. Fluid Mech.* **182**, 255–290.

Synge, J. L. 1933 The stability of heterogeneous liquids. *Proc. Trans. R. Soc. Can.* **27**, 1–18.

Ting, L. 1959 On the mixing of two parallel streams. *J. Math. Phys.* **38**, 153–165.

Wadey, P. D. 1991 On the nonlinear development of Görtler vortices in a compressible boundary layer. *Stud. Appl. Maths* **85**, 317–341.

Wadey, P. D. 1992 On the linear development of Görtler vortices in compressible boundary layers. *Eur. J. Mech.* B/*Fluids* **11**, 705–717.

Zhuang, M. 1999 The effects of curvature on wake-dominated incompressible free shear layers. *Phys. Fluids* **11**, 3106–3115.